

Supplement 1: A Model-Based Summary of Marquesan Archaeological Age Determinations

Barry V. Rolett and Thomas S. Dye

Contents

1	Introduction	4
1.1	Bayesian Calibration	4
1.2	Treatment of Marquesan Age Determinations	8
1.3	A Note on Table Column Names	16
2	Chronological Models for Marquesan Sites	17
2.1	Hanamiai Site, Tahuata Island	17
2.1.1	Outliers and Replicability of Hanamiai Solutions	19
2.1.2	Hanamiai Site Chronology	21
2.2	Hane Site, Ua Huka Island	22
2.2.1	Outliers and Replicability of Hane Solutions	25
2.2.2	Hane Site Chronology	27
2.3	Hakaea Beach Site, Nuku Hiva Island	27
2.3.1	Outliers and Replicability of Hakaea Beach Solutions	29
2.3.2	Hakaea Beach Site Chronology	30
2.4	Teavau'ua Coastal Flat, Nuku Hiva Island	31
2.4.1	Outliers and Replicability of Teavau'ua Solutions	32
2.4.2	Teavau'ua Site Chronology	33
2.5	Ho'oumi, Nuku Hiva Island	34
2.5.1	Ho'oumi Model	40
2.5.2	Outliers and Replicability of Ho'oumi Solutions	41
2.5.3	Ho'oumi Site Chronology	43
2.6	Ha'atuatua Site, Nuku Hiva Island	46
2.6.1	Outliers and Replicability of Ha'atuatua Solutions	48
2.6.2	Ha'atuatua Site Chronology	49
2.7	East Hanau, Hiva Oa Island	51
2.7.1	Outliers and Replicability of East Hanau Solutions	51
2.7.2	East Hanau Site Chronology	52

2.8	West Hanauī, Hiva Oa Island	54
2.8.1	Outliers and Replicability of West Hanauī Solutions	54
2.8.2	West Hanauī Site Chronology Summary	55
3	Marquesan Site Chronology Solutions	57
3.1	Robust Identification of Outliers	57
3.2	Replicability of Site Chronology Solutions	59
3.3	Effect of Local Marine Reservoir Correction	59
3.4	Relations of the Early Hanamiai Deposit	59
4	Marquesan Chronology	59
4.1	Polynesian Settlement History of the Marquesas	60
4.2	Material Culture Change	61
	References	68

List of Figures

1	Pragmatic overview of Bayesian chronology construction	8
2	Posterior outlier probabilities	13
3	Allen relations of two intervals	15
4	Residuality and intrusion at Hanamiai	18
5	Hanamiai phase boundaries, Conservative set	23
6	Hane phase boundaries, Conservative set	28
7	Hakaea phase boundaries, Conservative set	31
8	Teavau'ua phase boundaries, Conservative set	34
9	Ho'oumi phase boundaries, Conservative set	45
10	Ha'atuatua phase boundaries, Conservative set	50
11	East Hanauī age determinations, Conservative set	53
12	West Hanauī phase boundaries, Conservative set	56
13	Relation of Hanamiai I/II to other stratigraphic units	60
14	Marquesan settlement history	61
15	Hanamiai phase boundaries, Chronomodel calibration	65

List of Tables

1	Age determinations for Hanamiai site	20
2	Outliers identified by Hanamiai chronological solutions	20
3	Replicability of Heaton set Hanamiai site chronology solutions	20
4	Replicability of Burr set Hanamiai site chronology solutions	21
5	Replicability of Conservative set Hanamiai site chronology solutions	21

6	Variability in Hanamiai site chronology solutions	22
7	Summary statistics for Hanamiai site chronology solution	22
8	Age determinations for Hane site	24
9	Outliers identified by Hane chronological solutions	26
10	Replicability of Heaton set Hane site chronology solutions	26
11	Replicability of Burr set Hane site chronology solutions	26
12	Replicability of Conservative set Hane site chronology solutions	27
13	Variability in Hane site chronology solutions	27
14	Summary statistics for Hane site chronology solution	28
15	Age determinations for Hakaea Beach, Nuku Hiva	29
16	Replicability of Heaton set Hakaea site chronology solutions	29
17	Replicability of Burr set Hakaea Beach site chronology solutions	30
18	Replicability of Conservative set Hakaea Beach site chronology solutions	30
19	Variability in Hakaea Beach site chronology solutions	30
20	Summary statistics for Hakaea Beach site chronology solution	31
21	Age determinations for Teavau'ua Coastal Flat site	32
22	Replicability of Heaton set Teavau'ua site chronology solutions	32
23	Replicability of Burr set Teavau'ua site chronology solutions	33
24	Replicability of Conservative set Teavau'ua site chronology solutions . .	33
25	Variability in Teavau'ua site chronology solutions	33
26	Summary statistics for Teavau'ua site chronology solution	34
27	Age determinations for Ho'oumi site	42
28	Outliers identified by Ho'oumi chronological solutions	43
29	Replicability of Heaton set Ho'oumi site chronology solutions	43
30	Replicability of Burr set Ho'oumi site chronology solutions	43
31	Replicability of Conservative set Ho'oumi site chronology solutions . . .	44
32	Variability in Ho'oumi site chronology solutions	44
33	Summary statistics for Ho'oumi site chronology solution	44
34	Excluded Ha'atuatua age determinations	46
35	Age determinations for Ha'atuatua site	47
36	Outliers identified by Ha'atuatua chronological solutions	48
37	Replicability of Heaton set Ha'atuatua site chronology solutions	48
38	Replicability of Burr set Ha'atuatua site chronology solutions	49
39	Replicability of Conservative set Ha'atuatua site chronology solutions .	49
40	Variability in Ha'atuatua site chronology solutions	49
41	Summary statistics for Ha'atuatua site chronology solution	50
42	Age determinations for East Hanai site	51
43	Replicability of Heaton set East Hanai site chronology solutions	51
44	Replicability of Burr set East Hanai site chronology solutions	51
45	Replicability of Conservative set East Hanai site chronology solutions .	52
46	Variability in East Hanai site chronology solutions	52

47	Summary statistics for East Hanauī site chronology solution	52
48	Age determinations for West Hanauī site	54
49	Replicability of Heaton set West Hanauī site chronology solutions	54
50	Replicability of Burr set West Hanauī site chronology solutions	55
51	Replicability of Conservative set West Hanauī site chronology solutions	55
52	Variability in West Hanauī site chronology solutions	55
53	Summary statistics for West Hanauī site chronology solution	56
54	Summary statistics for Marquesan settlement history	61
55	Abundance, presence, and absence of temporally diagnostic artifacts	64
56	Summary statistics of Marquesan artifact traditions	66
57	Transition estimates with an Archaic transitional assemblage	67
58	Transition estimates with a Classic transitional assemblage	67
59	OxCal input files for the Marquesas calibrations	67
60	Chronomodel input files for the Marquesas calibrations	68

1 Introduction

This document presents the results of Bayesian calibrations designed to investigate the archaeological chronology of the Marquesas Islands in Eastern Remote Oceania. Bayesian calibrations carried out with OxCal software (Ramsey 1995) estimate chronologies for eight archaeological sites in the Marquesas, including six putative early sites—Hanamīai on Tahuata (Rolett 1998, 2021), Hane on Ua Huka (Sinoto 1968, 1970), and Ha’atuatua (Suggs 1961; Rolett and Conte 1995), Hakaea Beach (Allen and McAlister 2010), the Teavau’ua Coast Flat (M. S. Allen 2004), and Ho’oumi (Allen et al. 2021) on Nuku Hiva—and two later rockshelter sites at Hanauī on Hiva Oa (Sinoto 1979). Bayesian calibrations carried out with Chronomodel software (Lanos et al. 2015) estimate chronologies for temporally sensitive artifact types, including: (i) straight-shank one-piece fishhooks and curved or angular-shank one-piece fishhooks; (ii) trolling lure points in West and East Polynesian forms; (iii) tanged and untanged adzes; and (iv) two implements associated with breadfruit culture—poi pounders and cowrie-shell peelers.

The results yielded by the Bayesian calibrations provide the basis for a culture history of the Marquesas that estimates: (i) the date the Marquesas Islands were settled by Polynesians; (ii) the tempo of settlement establishment throughout the archipelago; (iii) chronologies for excavated stratigraphic units at eight dated sites; and (iv) the timing of cultural changes leading to the Classic Marquesan society described by Western explorers.

1.1 Bayesian Calibration

Bayesian calibration has been hailed as a revolution in archaeological chronology (e.g. Bayliss 2009; Bronk Ramsey 2008), its influence on the practice of archaeology in league

with two other widely recognized revolutions: (i) invention of the ^{14}C dating technique, whose adoption by archaeologists and widespread application to archaeological materials rewrote chronologies around the world; and (ii) development of atmospheric and marine calibration procedures for ^{14}C age determinations, which led to critical testing and often rejection of the diffusionist explanations that were mainstays of archaeological interpretation. Bayesian calibration, it is claimed, makes it possible for archaeologists to eschew fuzzy chronologies and engage in historical debate on timescales meaningful to the lived experiences of individuals in the past (Whittle et al. 2011; Whittle, Bayliss, and Healy 2010) and to correlate deposits at spatially discrete sites, even when these deposits represent relatively brief intervals (Bayliss, Farid, and Higham 2014). This promise of precision is potentially important for Pacific archaeologists investigating the settlement history of Eastern Remote Oceania—a history that was concealed for generations by fuzzy chronologies and which is now believed to have been episodic (Anderson et al. 2006), ‘pulse-like’ (Rieth and Cochrane 2018), or accomplished in a series of ‘explosive phases’ (Bellwood 2013, 197).

Bayesian calibration offers several advantages for investigating site and regional chronologies: (i) it is model-based, which facilitates communication and re-use; (ii) best practices have been developed to deal with sources of uncertainty often present in legacy data; (iii) software to carry out the calibrations is freely available; (iv) tests of model sensitivity to a variety of parameters can be carried out; (v) calibrations can be replicated to assess the stability of results; and (vi) the temporal intervals estimated for site phases can be compared and the nature of the relationship described precisely.

Archaeologists studying the settlement history of Eastern Remote Oceania have begun to explore the uses of Bayesian calibration (Dye 2011; Athens, Rieth, and Dye 2014; Dye 2015), but compared to some other parts of the world where Bayesian calibration is the norm (Bayliss 2015) uptake in the Pacific has been slow. How can Pacific archaeologists make better use of Bayesian calibration?

A useful step on the path to making better use of Bayesian calibration in Eastern Remote Oceania addresses the potential confusion introduced by the different meanings assigned to *calibration* in the practices of ^{14}C calibration and Bayesian calibration. In ^{14}C calibration, calibration refers to the calculation required to convert the decay rate of ^{14}C measured in the laboratory to the calendar timescale, taking into account fluctuations in the production of ^{14}C in the atmosphere and its subsequent diffusion through the atmospheric and marine ^{14}C reservoirs. Its goal is to estimate when the ^{14}C in a piece of dated organic material was removed from the atmospheric or marine ^{14}C reservoir. When applied conscientiously, it yields an estimate of when an organism was living, what the dendrochronologist Jeff Dean usefully labels the *dated event* (Dean 1978). In some situations, the age of the dated event might be directly useful to the archaeologist. For example, a bone recovered from an articulated pig skeleton buried at a Hawaiian *ahupua'a* land boundary (*ahupua'a* is translated literally as *pig altar*) might provide a useful estimate of when a land boundary consecration ritual was performed. True, the

^{14}C in the pig bone was taken out of the atmospheric and/or marine ^{14}C reservoir *before* the ritual. But the process that took the ^{14}C from its natural reservoir and incorporated it into the bone of the pig is reasonably believed to be on the order of a few years. Because this is shorter than the uncertainty of the ^{14}C dating technique as it is currently practiced, the estimated age of the pig bone is a reasonable estimate for the *ahupua'a* consecration ritual. In practice, however, the archaeologist is often interested in estimating the age of an event for which it proves impossible to recover directly associated dating material, or in the terms introduced by Dean (1978), when the dated event is not directly associated with the *target event*. In this case, ^{14}C calibration, which is solely concerned with the dated event and has no notion of the target event, can offer no help. In these cases and others, the Bayesian definition of calibration—as the calculation required to estimate the ages of two or more events whose ages relative to one another are known prior to the calibration—proves useful.

The Bayesian definition of calibration yields the archaeologist at least three benefits. First, the Bayesian definition is conceived in terms of chronologically related real-world events, whose ages can be estimated with information from a potentially wide range of sources. A single Bayesian calibration might incorporate ages estimated by ^{14}C , ^{230}Th , and optically stimulated luminescence, among others. Bayesian calibration can also incorporate dating information from the historic record, a feature that potentially connects archaeology directly to historical debates centered outside the discipline. In contrast, the ^{14}C definition of calibration is directly tied to the ^{14}C dating technique. Second, Bayesian calibration can estimate the ages of both dated events and target events, while ^{14}C calibration is limited to dated events. This capability expands the numbers and kinds of events whose ages can be estimated. In effect, Bayesian calibration renders the archaeological record a richer source of events than it would be otherwise.

Bayesian calibration estimates the ages of two or more events whose ages relative to one another are specified prior to the calibration in a chronological model based on stratigraphic observation, a material culture sequence, and/or expert opinion. Building a good chronological model that is both simple and includes as many target events as possible is an important step in the calibration because Bayesian calibration accepts the chronological model as true and uses it to deduce constraints for the calibration. The effort spent building a chronological model is often considerable, but it is repaid by the fact that such models ensure calibration results will be archaeologically interpretable (Buck, Cavanagh, and Litton 1996, 8), thus sparing the archaeologist the “Laocoön-like tangle of chronological problems” (Tuggle and Spriggs 2001, 171) often associated with interpreting individually calibrated ^{14}C age determinations in an ad hoc manner without the benefit of a chronological model. As archaeologists have gained experience with Bayesian calibration, and with the powerful software applications that carry out Bayesian calibration (Bronk Ramsey 2009a; Buck, Christen, and James 1999; Lanos et al. 2015), they have devised best practices to ensure the chronological model correctly reflects observations and expert opinion without over-determining calibration results.

For example, it is now possible to use a directed graph algorithm that generates a chronological model from stratigraphic observations made by the archaeologist, thus ensuring that the chronological model correctly reflects stratigraphic observations (Dye and Buck 2015).

A chronological model also makes it possible to identify outliers, which are a fact of life for most archaeological dating programs (Christen 1994). Outliers are especially common in legacy data sets from the Pacific, where many early excavations were undertaken in unconsolidated beach sand at coastal sites where material easily moves up and down the stratigraphic section. Because most dated material in legacy data sets was not explicitly associated with a particular activity, there is no way to determine *a priori* whether the age determination returned by the laboratory dates the intended target event, or if it is a residual or intrusive outlier. A second reason that legacy data sets in the Pacific often include outliers is that wood charcoal was not identified before it was sent to the dating laboratory, with the result that pieces of old wood—wood with substantial in-built age at the time it was deposited on the site—were sometimes dated. Unlike the problem of archaeological context, where residual material is older than the collection context and intrusive material is younger, the old wood problem always results in an age determination that is older than expected. Potential old wood charcoal might derive from burning wood from a long-lived tree such as *Cordia subcordata*, a useful small tree widespread in coastal environments and which can have an in-built age of 250 years or more (Allen and Huebert 2014, 258), or from burning driftwood, which might be several hundred years old before it washes ashore (Dye 2000). A third potential source of outliers comprises age determinations on marine shells that are not securely associated with the collection context. For example, shells are more or less common as natural constituents of beach sand and in some cases they may be as old as the beach itself. Thus, in dating marine shells care must be taken to identify shells that were deposited fresh and to avoid dating waterworn shells.

Finally, because there is no way to ensure that Bayesian calibration software has reported a solution in which all parameters have converged on the most likely estimate, replicability experiments should be carried out to ensure that “the results obtained for key parameters ... are the same to an appropriate level of accuracy” (Buck and Meson 2015, 575). These best practices figured into the design of the Bayesian calibration program reported here, which deals with a mix of modern and legacy data, some of it generated a half century ago.

A pragmatic overview of chronology building with Bayesian calibration identifies three inputs to the process (fig. 1). These include:

Chronological model the Bayesian prior that expresses known chronological information from one or more sources, typically including stratigraphic relations, material culture sequences, and expert opinion;

Age determinations typically ^{14}C age determinations reported by a standards compliant dating laboratory, but also potentially including age determinations with the ^{230}Th

or other dating methods; and

Treatments calibration variables, such as calibration curve, outlier model, boundary shape, among others, over which the chronologist exercises a choice.

There are three mutually exclusive outputs of Bayesian calibration, each of which is likely to occur one or more times during chronology construction. These include:

Outliers given a certain set of inputs, an outlier is an age determination that deviates from the range of expected values and which indicates an error of sufficient magnitude to degrade the accuracy of date estimates yielded by the calibration;

Unreplicable a calibration that does not identify outliers, but which yields date estimates that vary from run to run and are therefore not useful; and

Solution a calibration that runs without identifying outliers, is replicable, and which yields potentially useful date estimates.

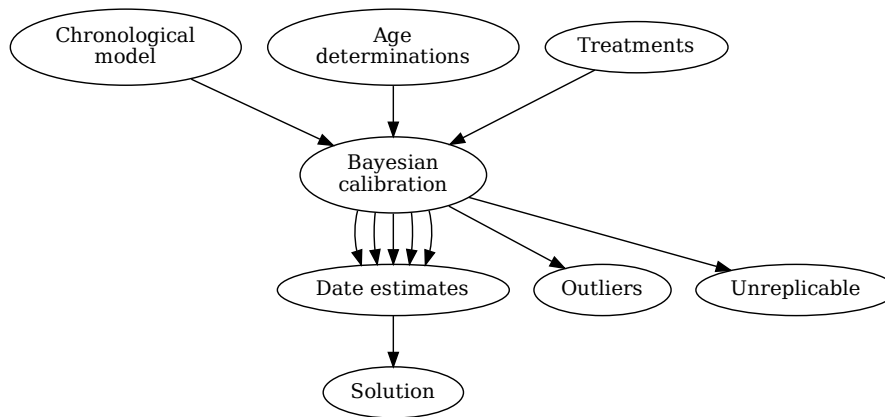


Figure 1: Pragmatic overview of Bayesian chronology construction.

In practice, outliers identified during chronology construction are either removed from the model or are modified in some way to reduce their influence on the results. For example, Christen (1994) proposed increasing the error term of age determinations identified as outliers. An unreplicable result indicates a mismatch between the model and data, and might indicate that the chronological model should be simplified. Replicable results, whose date estimates vary insubstantially from run to run, indicate a chronological solution that merits interpretation.

1.2 Treatment of Marquesan Age Determinations

The corpus of age determinations from Marquesan sites includes a variety of sample materials, many of which are from legacy or exploratory excavations with varying degrees of control over contextual integrity. In these circumstances outliers are expected and the

strategy used to identify them and compensate for their effect on the results plays a role in the design of the chronological model used in the Bayesian calibration.

The sample materials represented in the corpus of Marquesan age determinations include: (i) positively identified short-lived wood charcoal (Allen and Huebert 2014); (ii) positively identified long-lived wood charcoal; (iii) wood charcoal not positively identified but considered by the analyst to be comparable to a reference specimen; (iv) unidentified wood charcoal; and (v) marine shells of various kinds.

Positively identified long-lived wood charcoal, wood charcoal identified as comparable to a reference specimen, and unidentified wood charcoal have potential inbuilt age, which can make the age determination returned by the dating laboratory older—sometimes much older—than the cultural activity the archaeologist hopes to date. In some cases, care must be taken to control for the potential effects of in-built age (e.g., Dye 2000).

Marine shells take their carbon from near the surface of the marine ^{14}C reservoir, which has an apparent age that models indicate is about four centuries older than the atmospheric ^{14}C reservoir, with local variations that depend on currents and up-welling (Stuiver, Pearson, and Braziunas 1986). These local variations are handled in ^{14}C dating by applying a ΔR correction, which is typically determined by dating marine materials of known age and comparing the known age with the ^{14}C age determination. The ocean reservoir model was changed recently, and values of ΔR calculated for the old model must be re-calculated for the new model (Heaton et al. 2020). Heaton et al. (2020) propose a value of $\Delta\text{R} -20 \pm 39$ for the Marquesas based on radiocarbon dates from modern, pre-bomb corals of known age (Burr et al. 2009). A range of other ΔR estimates have been proposed for the Marquesas, some of which are based on “paired” archaeological samples rather than known-age materials. Among the ΔR estimates that have been proposed for the Marquesas: (i) -16 ± 58 was derived for the old marine reservoir model from a set of “paired” charcoal and marine shell samples from TP8 and TP9 at the Teavau’ua site on Nuku Hiva (Petchey et al. 2009, 2240) and has not been recalculated for the new marine reservoir model; (ii) 38 ± 28 was also derived for the old marine reservoir model from “paired” charcoal and marine shell samples collected from TP5, TP8, and TP11 at the Teavau’ua site on Nuku Hiva—in this case, the estimate is based on pooled ^{14}C age determinations on two marine shells and three of six pieces charcoal that most closely matched the shell dates calibrated with a ΔR of 45 ± 48 (Petchey et al. 2009, 2240)—and the value has been recalculated for the new marine reservoir model as -83 ± 31 (Allen et al. 2021, 86); (iii) -136 ± 65 was derived for the new marine reservoir model based on an estimate of temporal variability in the apparent age of the marine reservoir in the South Pacific (Petchey 2020) and has been applied to materials that date to the second half of the last millennium (Allen et al. 2021, 86); (iv) -262 ± 28 was derived for the new marine model based on “paired” charcoal and marine shell samples from a fire feature assumed to represent a brief interval, as discussed further below, and is applied to materials that date to the first half of the last millennium (Allen et al. 2021, 86); (v) 109 ± 39 is derived for the old marine reservoir model from one of the 26 ^{14}C

measurements on coral reported by Burr et al. (2009)—which might be problematic (see Allen et al. 2021, 86)—and has been recalculated as -20 ± 39 for the new marine reservoir model (Heaton et al. 2020); (vi) 45 ± 48 was derived for the old marine reservoir model by Petchey et al. (2009, 2237) from 24 of the ^{14}C measurements on coral reported by Burr et al. (2009) and is recalculated here as -81 ± 38 for the new marine reservoir model using all 26 of the ΔR values calculated from Burr et al. (2009) using the mean error of the reported values; and (vii) -81 ± 10 is derived here for the new marine reservoir model based on all 26 of the ΔR values calculated from Burr et al. (2009) using the standard error of the mean.

Taking these various estimates into consideration, we designed three sets of chronological models, which initially differed only in the value of ΔR applied to marine samples. The first set of chronological models, referred to hereafter as the Heaton set, follows the recommendation of Heaton et al. (2020) and applies a ΔR value of -20 ± 39 . The second set, referred to hereafter as the Burr set, takes into account the issue raised by Allen et al. (2021, 86) and applies a value of -81 ± 10 , which translates the reservoir age calculated by Burr et al. (2009) to the new marine reservoir model. The third set, referred to hereafter as the Conservative set, applies a ΔR value of -81 ± 38 , which differs only in the error term calculated as the mean error of the individual age determinations used to estimate the reservoir age.

Based on a number of concerns, the decision was taken not to model two other ΔR proposals for the Marquesas because they lack sufficient empirical warrant. The ΔR value of 38 ± 28 proposed by Petchey et al. (2009) was not modeled because it is based on “paired” charcoal and marine shell samples collected at three discontinuous locations from a context with a relatively long duration, a situation that represents a weak basis for establishing the contemporaneity required to calculate ΔR accurately. In the case of the Teavau‘ua site, the modeling reported below estimates an approximately century-long duration of the contexts assigned to Layer IV, from which the “paired” samples were collected (table 26), whereas the difference between the proposed ΔR value and the estimates in the Heaton, Burr, and Conservative sets is less than the context duration. The true ages of very many pieces of shell recovered from Layer IV will differ from the true ages of the great majority of other materials recovered from the layer by more than this difference. Thus, a difference greater than this in “paired” age determinations from Layer IV is expected, even in the absence of any difference in ΔR . There is no way to know if ΔR even factors into the estimate. An archaeological chronology that uses the ΔR value of 38 ± 28 will show little difference from one that uses a ΔR estimate from among the Heaton, Burr, and Conservative sets.

The ΔR value of -16 ± 58 proposed by Petchey et al. (2009) is based on a pair of age determinations from Layer IIIb of the Teavau‘ua site. It is not modeled because it, too, claims to have detected a ΔR value that differs from the estimates in the Heaton, Burr, and Conservative sets by less than the estimated duration of Layer IIIb. Thus, the observed differences in “paired” age determinations from Layer IIIb is not unusual, even in the

absence of any difference in ΔR . As with the “paired” samples from Layer IV at the Teavau’ua site, there is no way to know if ΔR even factors into the estimate based on “paired” samples from Layer IIIb. An archaeological chronology that uses the ΔR value of -16 ± 58 might show substantial differences from one that uses a ΔR estimate from among the Heaton, Burr, and Conservative sets.

The ΔR value of -262 ± 28 , which was proposed by Allen et al. (2021) to calibrate an age determination on marine shell from the fill of a pit interpreted as a hearth at the Ho’oumi site, is not modeled here. The excavators’ expectation that materials recovered from the pit fill relate to use of the hearth at a point in time led them to derive a ΔR value that ensures the calibrated age of the marine shell closely approximates the ages of two out of three age determinations on wood charcoal. The rationale for the decision not to model this ΔR value includes: (i) an alternative depositional analysis of the pit feature and its fill material based on the principles of archaeological stratigraphy (Harris 1989); and (ii) acknowledgment that pit fill typically includes materials of disparate ages.

The excavators calculated a ΔR value of -262 ± 28 using three of the four age determinations on short-lived materials—two on wood charcoal in addition to the one on marine shell—recovered from the fill of the basin-shaped Feature 1 hearth exposed in the wall profile of Trench 4. The fourth age determination on short-lived material recovered from Feature 1, a piece of *C. nucifera* endocarp charcoal dated as Beta-303443, provided an age determination that is quite a bit younger than the other two age determinations on charcoal. The excavators rejected Beta-303443 and excluded it from their analysis, presumably because it is at odds with the expectation that materials in the fill should relate solely to use of the pit at a point in time. Nevertheless, the excavators’ expectation that Feature 1 represents a brief interval is problematic because the Feature 1 hearth is not a single context as the excavators contend, but instead includes the interfacial context that represents the pit cutting event and at least one fill context deposited subsequent to the cutting. In our view, it is important to consider the likelihood that pits such as Feature 1 typically fill with material nearby the pit, some of which was deposited when the pit was excavated and older materials were likely brought to the surface. In this situation, residual charcoal in pit fill is to be expected and is reflected in the three older dates. On this account: (i) the date most nearly contemporaneous with the cutting interface would, in fact, be the date on the material rejected by the excavators, Beta-303443; (ii) the Feature 1 fill contains a mix of materials of different age, with a range of about 2 centuries; and (iii) there is no warrant for deriving a ΔR value of -262 ± 28 .

Finally, temporal change in ΔR was not modeled because this is an active area of research with considerable evidence for regional stability (Burr et al. 2009; Paterne et al. 2004; Petchey et al. 2009). In addition, the argument for variation over time is at a nascent stage (Petchey 2020; Petchey and Schmid 2020). There are two aspects of the temporal change model that would seem to require additional modeling prior to its application to Marquesan archaeology.

- Although the model for temporal change in ΔR was developed for the southwest

Pacific, its application to other parts of the Pacific is not well established (Komugabe-Dixon et al. 2016, 982). Further work is needed to demonstrate that the model is relevant for islands in the Central Pacific, including the Marquesas.

- The exploratory work of Petchey and Schmid (2020), which attempts to generalize the southwest Pacific findings to New Zealand, uses “paired” samples that derive from archaeological contexts with unspecified duration, which potentially violates the contemporaneity required to calculate ΔR with paired samples. The effects of errors potentially introduced by the failure to control for contemporaneity are magnified when the authors divide the sequence into several periods, which restricts sample sizes.

The chronological models developed here all follow the same conventions.

A Southern hemisphere atmospheric calibration curve is used for two reasons: (i) the Marquesas Islands are located between 8° and 10.5° south of the Equator, and (ii) previously, Petchey et al. (2009, 2238) argued that a Northern hemisphere atmospheric calibration curve should be applied to Marquesan ^{14}C age determinations, however in more recent work the same authors (Allen et al. 2021) use the Southern hemisphere calibration curve.

In the OxCal calibrations, outliers were identified and treated as recommended by Christen (1994) using the OxCal outlier model, `SSimple` (Bronk Ramsey 2009b). An initial run using all of the age determinations applied the `SSimple` outlier model with an uninformative prior probability of 0.05. The distribution of posterior outlier probabilities, which in each case had a long tail of high values, was examined to determine a cut-off value of 0.10 for outliers (fig. 2). Age determinations with a posterior outlier probability greater than the cut-off value were removed from the calibration. A second calibration, excluding the outliers identified in the initial run, yielded posterior outlier probabilities without a long tail of high values that might be interpreted as strong evidence for additional outliers. Outliers with posterior probabilities greater than 0.10 were not removed from the calibration at this stage. This calibration was run five times to determine whether or not it yielded stable results for parameters of interest (Buck and Meson 2015). Results of replicable calibrations are considered chronology solutions with interpretable date estimates for modeled events. It should be noted that the A statistics calculated by OxCal are not reliable when an outlier model is used; the fact that many of the calibrations yielded A statistics less than the rule-of-thumb threshold of 60 is not a concern.

Chronology solutions for the settlement-era sites were compared with one another to determine the basic relations of inter-site time intervals represented by selected stratigraphic units. The comparisons were carried out with reference to the Allen algebra, which was designed to maintain knowledge about temporal intervals (J. F. Allen 1983). The Allen algebra identifies thirteen basic relations between two definite intervals, each of which is labeled descriptively (fig. 3). The thirteen basic relations exhaust the possibilities for two definite intervals. Note that Allen relations do not consider the magnitude

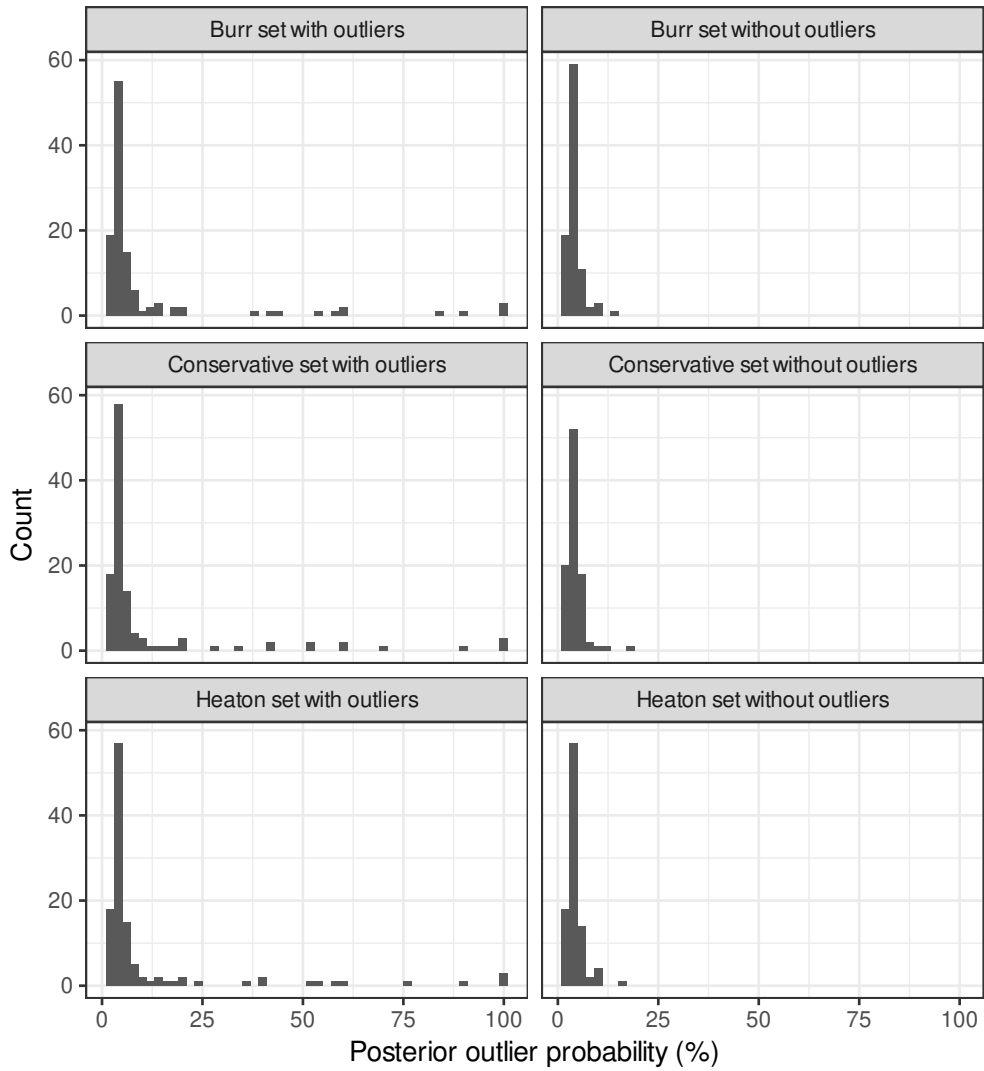


Figure 2: Posterior outlier probabilities of Marquesan age determinations before and after outlier removal. Note that most values are close to the uninformative prior of 5%.

of differences between two intervals, but focus solely on their basic relations.

The use of Allen relations can be illustrated by the hypothetical example of a burnt fishhook excavated from a hearth. If we assume that charring of the fishhook occurred in the hearth, Allen algebra can express relations for the sequence of events beginning with fabrication of the fishhook and ending when the fishhook was tossed into the fire. In this example, a is the time the fishhook was made, and b is when a fire was burning in the hearth. A likely set of relations is that a precedes b (the fishhook was made before the fire, with a time gap separating these two events). Another possibility is that a overlaps with b . In other words: 1) shaping the fishhook began before the fire was lit, and 2) the fishhook was finished and tossed into the hearth while the fire was burning. But we can rule out the possibility that a is overlapped by b . This is because if the fire stopped burning before the fishhook was finished, there is no way to explain the charring. By contrast, if the fishhook was fabricated while the fire was burning and tossed into the hearth before the fire stopped, we can say a occurred during b . However, it is not possible that a contains b , meaning that shaping the fishhook started before the fire was lit and the fishhook was tossed into the hearth after the fire stopped burning. Once again, this set of relations cannot explain the charring. We could continue to explain the full set of Allen relations but these are the ones needed to understand the chronological relationship between Hanamiai and other sites in our study.

The tempo of site establishment in the Marquesas was calculated using the R statistical software package `ArchaeoPhases` (Philippe and Vibet 2019), which post-processes the Markov Chain simulated by the Bayesian calibration applications commonly used by archaeologists. In addition to the various statistical functions, which were used to create most of the tables in this document, and the plotting functions, which were used to create most of the figures, the `ArchaeoPhases` software includes functions designed to estimate joint probability distributions. One of these, `OccurrencePlot`, is used to estimate the tempo of site establishment in the Marquesas. In this case, `OccurrencePlot` was used to investigate the joint probability of site establishment events estimated by the site chronology solutions, yielding estimates of when the first and subsequent sites were established in the Marquesas. This approach to the problem of estimating the age of the first site to be established in a region differs from the one traditionally adopted by archaeologists that seeks to identify and date the earliest site. Instead, the `OccurrencePlot` function ignores which site was responsible for a site establishment event in the Markov Chain simulation, in order to estimate when the first and subsequent sites were established. Its focus is regional, rather than site-based. Instead of asking the question, “Which site was the first to be established in the Marquesas?”, the `OccurrencePlot` answers the question, “When was the first site established in the Marquesas?”

The `Chronomodel` application, rather than `OxCal`, was used to estimate artifact chronologies for the reasons elaborated by Banks et al. (2019, 192, 197): (i) the `Chronomodel` application avoids the unnecessary introduction of additional priors

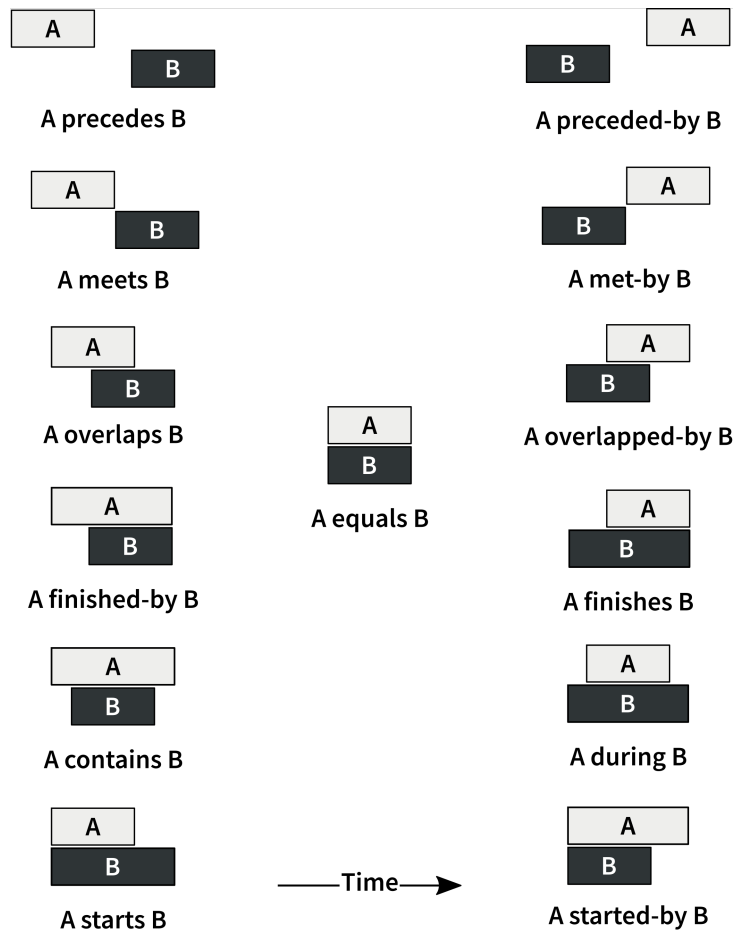


Figure 3: Allen relations of two intervals, A and B, and the labels used to identify and describe them. Note that the relations in the right column are the converses of the relations in the left column. *After: Alspaugh (2019, Table 1).*

that is unavoidable with `OxCal` when attempting to construct regional chronologies with data from multiple stratified sequences; (ii) the inclusion of stratigraphic sequences that are not dated from top to bottom is not problematic because all the individual sequences are nested within the broad cultural phase structure, which covers the entire period of interest and is associated with its own stratigraphic constraints; (iii) with `Chronomodel` one is not limited to using ^{14}C ages from stratified sequences because age measurements from taphonomically reliable and culturally diagnostic single component sites can be included in the cultural phase portion of the model, which makes it possible to take into account all relevant data when constructing a regional age-model of archaeological cultures.

A desirable feature of a model-based approach to estimating chronologies, such as Bayesian calibration, is that the models can easily be exchanged among investigators. Independent investigators can calibrate the models to ensure that published results are reproducible, and they may also choose to use them as a basis for new work that aims to augment, refine, and/or reinterpret calibration results. To this end, the `OxCal` and `Chronomodel` input files for the calibrations reported here are provided as PDF file attachments in Section [Input Files](#). When this document is opened with a PDF reader that recognizes file attachments, clicking on one of the links provided will extract the input file as a text document that can be studied and saved for future use, as appropriate.

1.3 A Note on Table Column Names

This document includes tables that summarize Bayesian calibration results (e.g., table 7) and assess the variability in results (e.g., table 6) and replicability of site chronology solutions for the Marquesan sites (e.g., table 3). These tables use the following abbreviations to label statistics summarized in the columns:

mean mean value of the MCMC chain;
sd standard deviation of the mean value of the MCMC chain;
min minimum value of the MCMC chain;
q1 first quartile of the MCMC chain;
median median value of the MCMC chain;
q3 third quartile of the MCMC chain;
max maximum value of the MCMC chain;
ci.inf lower credible interval of the MCMC chain at 95 percent; and
ci.sup upper credible interval of the MCMC chain at 95 percent.

This document also includes tables that list the ^{14}C age determinations for each of the sites (e.g., table 1). These tables include a column labeled “ θ ” that identifies the dated event (Dean 1978), another labeled “Context” that refers to the unit within which age determinations are grouped in the Bayesian prior, and a third labeled “CRA”, that refers to the conventional radiocarbon age (Stuiver and Polach 1977). Note that the unit represented by Context might be identified by the excavator as a layer, phase, or some other name. The accompanying text should indicate the nature of the correspondence.

2 Chronological Models for Marquesan Sites

This section describes chronology solutions yielded by Bayesian calibrations carried out for eight Marquesan archaeological sites, including the Hanamiai site on Tahuata, the Hane site on Ua Huka, the Hakaea Beach, Teavau'ua Coastal Flat, Ho'oumi, and Ha'atuatua sites on Nuku Hiva, and the East and West Hanau sites on Hiva Oa. The Hanamiai site is reviewed first, because it is central to the main paper. The other sites are reviewed in no particular order.

Three chronology solutions were achieved for each site using different ΔR treatments of the radiocarbon age determinations. Each of the site chronology solutions is described here, together with an overview of the site's excavation, stratification, and dating program. Additional background information for the sites can be found in Supplement 2. In some cases, the proposed site chronology solution uses a sequence that differs from the published sequence, typically by lumping stratigraphic units when the resolution of available ^{14}C dating and other evidence is insufficient to establish these units as chronologically distinct deposits. This is the case for Hanamiai, Hane, and Ho'oumi. As might be expected in a synthesis such as this, which incorporates results reported by several investigators over half a century, terminology and naming protocols for stratigraphic units and phases vary considerably, with the potential to confuse the reader. This document follows the published sources wherever possible, despite the potential for confusion. Outliers identified by the calibrations are described, along with the likely cause of their poor fit to the model and other data, and evidence is provided for the replicability of calibration results. Finally, the variability introduced by different ΔR treatments is assessed, leading to the choice of chronological model, which is summarized with statistics for phase boundaries generated by software routines included in the `ArchaeoPhases` package (Philippe and Vibet 2019). Section [Input Files](#) presents the `OxCal` and `Chronomodel` input files used to produce the reported calibrations.

2.1 Hanamiai Site, Tahuata Island

Hanamiai is a coastal dune site with a continuous series of cultural deposits extending to depths of more than 2.5 m below surface. See the main text for site and project background information. The Hanamiai archaeological sequence is defined using a nomenclature consisting of stratigraphic layers labelled A, B, C and so on, where A refers to the youngest deposit. The nomenclature also includes cultural phases numbered I through V, with V referring to the youngest phase and I referring to the oldest. In the following discussion, numbers for these cultural phases, which were used to group artifacts and faunal assemblages for quantitative analysis, also denote the calendrical phases used in the Bayesian models for this study. The Hanamiai V deposits yield numerous nineteenth century Euro-American artifacts.

The Hanamiai site consists mainly of unconsolidated calcareous marine sand deposits, where residuality and intrusion of cultural materials, two problems that Bayesian calibra-

tion has exposed as common in archaeological deposits (Bayliss and Ramsey 2004, 33), are expected. At Hanamiai, the potential scope of these problems can be apprehended by the stratigraphic distribution of distinctive chips from the manufacture of a unique whale bone implement found 246 cm below datum (fig.4). The whale bone chips were found at depths ranging from 210–215 cm to 260–265 cm below datum. Most of them are residual in the 35 cm of deposit overlying the whale bone implement, while others are intrusive to a depth of 15 cm below the implement.

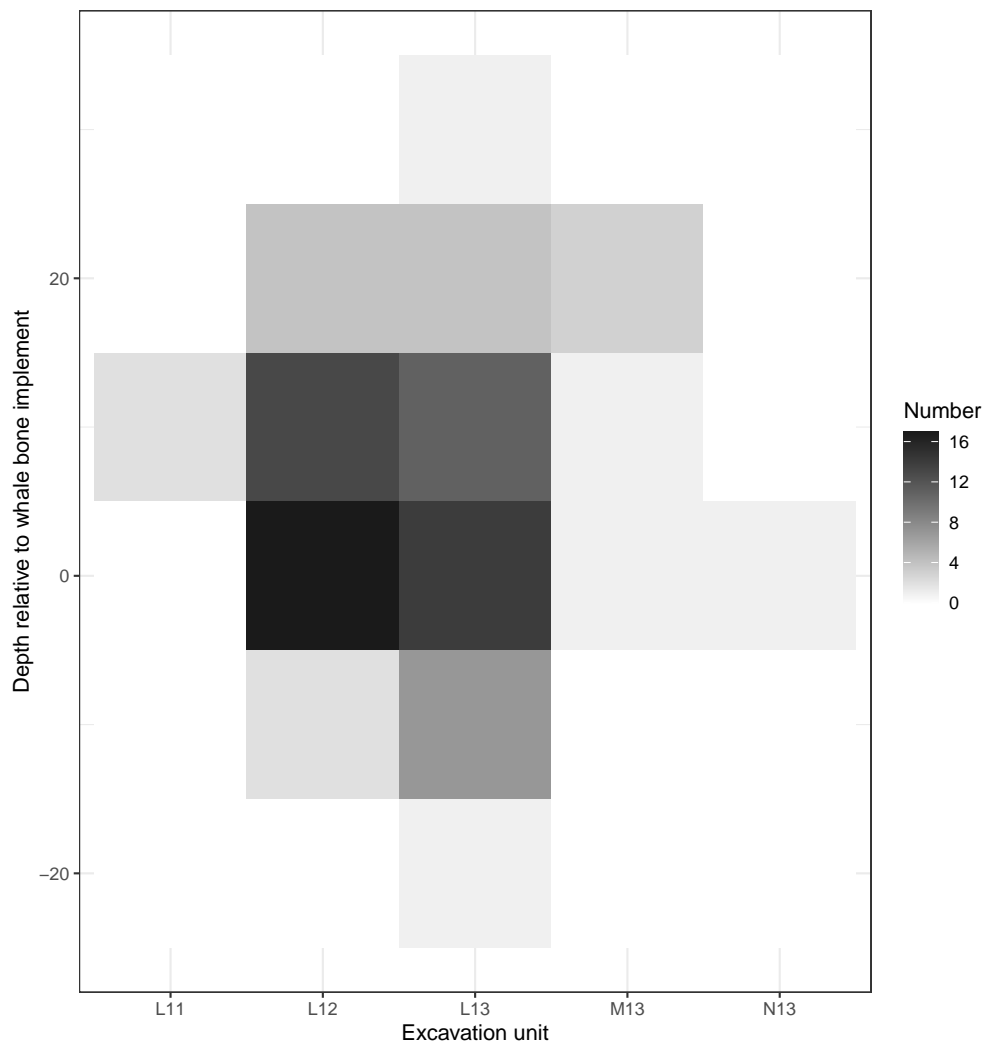


Figure 4: Residuality and intrusion at Hanamiai. Stratigraphic distribution of distinctive chips from a unique whale bone implement recovered at 246 cm below datum.

In response to the difficulties introduced by residuality and intrusion a ^{14}C calibration might achieve a good fit between data and model either by (i) “rejecting” some of

the data, or (ii) consolidating excavated strata to simplify the stratigraphic sequence. The decision was taken to simplify the stratigraphic sequence to take into account the demonstrated potential for residuality and intrusion. This was achieved by consolidating cultural phases I and II and treating them as a single unit, I/II. The chronological model based on the simplified stratigraphic sequence can be expressed algebraically (eq. 1), where α_n is the calendar date of the start of phase n , β_n is the calendar date of the end of phase n , and Θ_n are the calendar dates of the dated events assigned to phase n . Note that outliers removed from a calibration to achieve a site chronology solution are called out in the text. The floating parameter, 1950, is the 0 year for ^{14}C calibration.

$$\alpha_{\text{I/II}} > \Theta_{\text{I/II}} > \beta_{\text{I/II}} \geq \alpha_{\text{III}} > \Theta_{\text{III}} > \beta_{\text{III}} \geq \alpha_{\text{IV}} > \Theta_{\text{IV}} > \beta_{\text{IV}} \geq \alpha_{\text{V}} > \theta_{66} > \beta_{\text{V}} \geq 1950, \quad (1)$$

where

$$\Theta_{\text{I/II}} = (\theta_1, \theta_2, \theta_3, \theta_4, \theta_5, \theta_6, \theta_7, \theta_9, \theta_{10}, \theta_{11}, \theta_{12}, \theta_{13}, \theta_{14}, \theta_{65}, \theta_{67}), \quad (2)$$

$$\Theta_{\text{III}} = (\theta_8, \theta_{120}), \quad (3)$$

and

$$\Theta_{\text{IV}} = (\theta_{119}, \theta_{121}, \theta_{122}). \quad (4)$$

The Hanamiai site chronology is based on 22 age determinations made on a variety of materials (table 1). The age determinations estimate the dates of 21 events, which are labeled with an identifier unique to this analysis in column “ θ ”. Note that two of the age determinations estimate the age of event θ_8 . Seven age determinations were made on unidentified wood charcoal collected from fire-features ranging from earth ovens to burn surfaces, in addition to isolated charcoal fragments collected from the sediment matrix. Five age determinations were made on wood charcoal identified as *Calophyllum inophyllum*, *Cocos nucifera*, or *Cordia subcordata*. All of the age determinations on wood charcoal have potential for in-built age and none are from short-lived taxa (Allen and Huebert 2014). Three age determinations on coconut shell are considered short-lived, as are seven age determinations on pieces of worked pearl shell.

2.1.1 Outliers and Replicability of Hanamiai Solutions

The three chronological solutions for Hanamiai identify two outliers from Hanamiai I and II (table 2). Beta-363627 and Beta-17468 date pieces of wood charcoal that are too old for their contexts according to the model and data, likely due to in-built age.

Hanamiai Heaton Set Solution Various measures of boundary estimates for Hanamiai (table 3) vary by 11 or fewer years over five calibrations that use the ΔR value recommended by Heaton et al. (2020). This result indicates that the calibration is replicable.

Table 1: Age determinations for Hanamiai site

θ	Context	Laboratory	CRA	Material	Reference
1	I	Beta-363627	920 \pm 30	<i>C. inophyllum</i> wood charcoal	this paper
2	I	Beta-363628	850 \pm 30	<i>C. subcordata</i> wood charcoal	this paper
3	I/II	Beta-15567	850 \pm 60	<i>C. nucifera</i> wood charcoal	Rolett (1998, 84)
4	I	Beta-363630	840 \pm 30	<i>C. inophyllum</i> wood charcoal	this paper
5	I	AA 2820-V3738	890 \pm 80	isolated charcoal	Rolett (1998, 84)
6	I	AA 2819-V3737	790 \pm 80	charcoal from burnt surface	Rolett (1998, 84)
7	II	AA 2822-V3740	870 \pm 80	charcoal from hearth	Rolett (1998, 84)
8	III	AA 2821-V3739	660 \pm 80	charcoal from hearth	Rolett (1998, 84)
8	III	Beta-15566	620 \pm 90	charcoal from hearth	Rolett (1998, 84)
9	I	Beta-436909	1040 \pm 30	worked pearl shell	this paper
10	II	Beta-436910	1140 \pm 30	worked pearl shell	this paper
11	II	Beta-436911	1070 \pm 30	worked pearl shell (burnt)	this paper
12	I	Beta-363631	660 \pm 30	<i>C. nucifera</i> endocarp charcoal	this paper
13	I	Beta-436912	740 \pm 30	<i>C. nucifera</i> endocarp charcoal	this paper
14	II	Beta-436913	770 \pm 30	<i>C. nucifera</i> endocarp charcoal	this paper
65	II	Beta-17468	1250 \pm 100	charcoal from hearth	Rolett (1998, 84)
66	V	Beta-15565	130 \pm 100	charcoal from earth oven	Rolett (1998, 84)
67	II	Beta-363629	750 \pm 30	<i>C. nucifera</i> wood charcoal	this paper
119	IV	Beta-626054	710 \pm 30	worked pearl shell	this paper
120	III	Beta-626055	1050 \pm 30	worked pearl shell	this paper
121	IV	Beta-626056	700 \pm 30	worked pearl shell	this paper
122	IV	Beta-626057	980 \pm 30	worked pearl shell	this paper

Table 2: Outliers identified by Hanamiai chronological solutions

θ	Laboratory	Cause	Heaton	Burr	Conservative
1	Beta-363627	old wood	✓	✓	✓
65	Beta-17468	old wood	✓	✓	✓

Table 3: Replicability of Heaton set Hanamiai site chronology solutions

	mean	q1	median	q3	ci.inf	ci.sup
Hanamiai I and II start	2	2	2	2	4	3
Hanamiai I and II end	1	1	1	1	2	1
Hanamiai III start	1	1	0	0	1	1
Hanamiai III end	1	0	1	1	4	4
Hanamiai IV start	0	1	1	0	6	6
Hanamiai IV end	3	3	3	3	5	2
Hanamiai V start	5	7	6	5	5	3
Hanamiai V end	7	11	8	5	8	0

Hanamiai Burr Set Solution Various measures of boundary estimates for Hanamiai (table 4) vary by 17 or fewer years over five calibrations that use a ΔR estimate based on Burr et al. (2009). This result indicates that the calibration is replicable.

Table 4: Replicability of Burr set Hanamiai site chronology solutions

	mean	q1	median	q3	ci.inf	ci.sup
Hanamiai I and II start	2	3	2	1	2	1
Hanamiai I and II end	1	1	1	1	1	1
Hanamiai III start	1	1	0	0	2	2
Hanamiai III end	1	0	0	1	6	7
Hanamiai IV start	1	1	2	1	5	4
Hanamiai IV end	4	6	5	4	10	6
Hanamiai V start	7	11	7	5	10	4
Hanamiai V end	10	15	9	3	17	0

Hanamiai Conservative Set Solution Various measures of boundary estimates for Hanamiai (table 5) vary by 18 or fewer years over five calibrations that use a ΔR estimate based on Burr et al. (2009) incorporating a conservative estimate of the error. This result indicates that the calibration is replicable.

Table 5: Replicability of Conservative set Hanamiai site chronology solutions

	mean	q1	median	q3	ci.inf	ci.sup
Hanamiai I and II start	2	2	1	1	6	1
Hanamiai I and II end	1	1	1	1	2	1
Hanamiai III start	0	1	0	0	2	1
Hanamiai III end	1	0	1	2	5	6
Hanamiai IV start	2	3	2	2	2	6
Hanamiai IV end	6	6	7	6	9	7
Hanamiai V start	9	13	9	9	11	6
Hanamiai V end	12	18	15	8	13	0

2.1.2 Hanamiai Site Chronology

The value of ΔR in the calibration introduces variability of 15 or fewer years in measures of boundary estimates for Hanamiai (table 6). Most of the variation is concentrated in Hanamiai V. Elsewhere, the variation is less than a decade. These results indicate that ΔR has little effect on parameter date estimates. In this case, any one of the three chronology solutions might be used to summarize the chronology of the Hanamiai site.

The Conservative set solution is chosen to estimate Hanamiai site chronology (table 7, fig. 5). The 95% credible interval for site establishment is AD 1160–1266. The earliest phase, identified as Hanamiai I and II, ends in AD 1314–1415. The succeeding phase, Hanamiai III, was laid down during a relatively brief interval between AD 1340–1440 and

Table 6: Variability in Hanamiai site chronology solutions

	mean	q1	median	q3	ci.inf	ci.sup
Hanamiai I and II start	3	3	3	2	4	1
Hanamiai I and II end	1	1	1	1	0	0
Hanamiai III start	1	1	0	0	0	0
Hanamiai III end	1	0	0	1	4	4
Hanamiai IV start	2	2	2	2	6	7
Hanamiai IV end	4	5	5	4	8	7
Hanamiai V start	7	11	8	7	11	6
Hanamiai V end	10	15	10	5	12	0

AD 1375–1582. The Hanamiai IV phase starts in AD 1435–1701 and ends in AD 1650–1880. The Hanamiai V phase begins in AD 1693–1932 and ends in AD 1738–1951.

Table 7: Summary statistics for Hanamiai site chronology solution

	mean	sd	min	q1	median	q3	max	ci.inf	ci.sup
Hanamiai I and II start	1218	29	1096	1203	1222	1239	1279	1160	1266
Hanamiai I and II end	1366	26	1281	1347	1368	1385	1478	1314	1415
Hanamiai III start	1393	25	1287	1378	1394	1410	1511	1340	1440
Hanamiai III end	1460	53	1327	1424	1449	1487	1758	1375	1582
Hanamiai IV start	1573	72	1348	1520	1576	1626	1809	1435	1701
Hanamiai IV end	1755	60	1526	1713	1753	1796	1945	1650	1880
Hanamiai V start	1813	65	1544	1769	1817	1862	1949	1693	1932
Hanamiai V end	1868	63	1625	1831	1882	1920	1953	1738	1951

2.2 Hane Site, Ua Huka Island

Attempts to establish a chronology for the Hane site began in the 1960's when ¹⁴C dating laboratories often underestimated sample standard deviations (Baillie 1990) and archaeologists typically paid little or no attention to provenance, composition, statistical, experimental, or systemic factors now recognized as important in the evaluation of ¹⁴C data (Taylor 1987, 105–146). The site was since re-dated twice with better results, but still with uncertainties that complicate evaluation. The two recent Hane dating projects include a reinterpretation of the original Hane sequence (Anderson and Sinoto 2002), and a subsequent excavation adjacent to the original one (Conte and Molle 2014).

Sinoto excavated in two areas in the central portion of the site, which he labeled Area A and Area B. The deposits in Areas A and B have been correlated by classifying excavation stratigraphic units as belonging to either the Upper levels or the Lower levels.

However, the stratigraphy can be divided broadly for the purposes of analysis into two groups; the lower levels (V, VI, VII in Area B, which, in the center of the main mound, are associated with the lower pavement, and beneath it; Levels II to VI in Area A), and the upper levels which are Level I in Area A

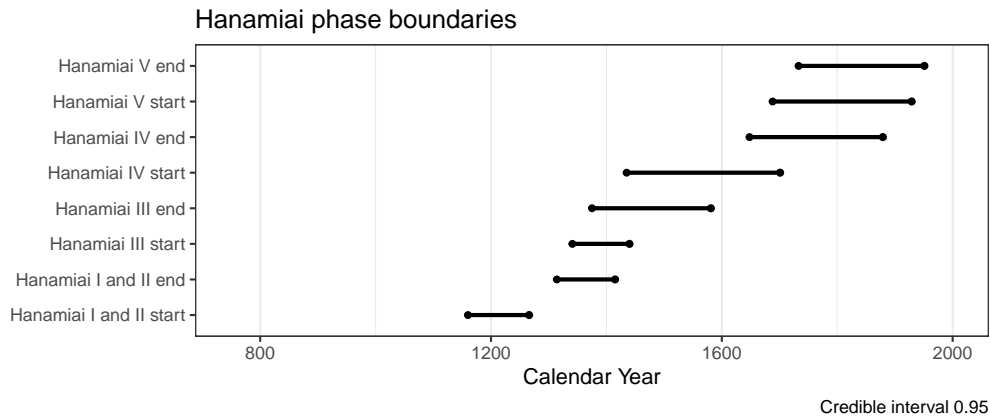


Figure 5: Hanamiai phase boundaries, Conservative set.

and Levels I–IV in Area B. Whether Level VII should be regarded as separate from Level VI was questioned by Anderson (1994) and it is not regarded now by Sinoto as a discrete layer. (Anderson and Sinoto 2002, 249–251)

Anderson and Sinoto (2002) report 14 previously published age determinations and 10 new age determinations for Hane. They exclude the statistically modern results of four age determinations (Gak-528, -933, -935, and -936); these age determinations are also excluded from the analysis reported here. Their list includes 22 age determinations for the lower levels and two age determinations for the upper levels (table 8). The age determinations include 14 on pieces of unidentified charcoal and another on a composite sample reported as “turtleshell etc.” with potential for in-built age and seven on marine shells that have been classified as short-lived. The age determinations from the upper level include one on pearl shell, θ_{58} , classified as short-lived, and another on unidentified charcoal, θ_{63} , with potential for in-built age.

The Hane site was re-investigated in 2009 with excavation of 18 m² in a block at the northwest end of Area B (Conte and Molle 2014). This excavation revealed an upper and a lower pavement, which makes it possible to correlate the newly excavated stratification with the upper and lower levels identified by Anderson and Sinoto (2002); nevertheless, it is not possible to correlate the stratigraphic sequence identified in 2009 with Sinoto’s excavations, which extended over a larger area of the dune (Conte and Molle 2014, 130). Seventeen age determinations are reported, including ten on wood charcoal and seven on human bone (Conte and Molle 2014, 129). The age determinations on human bone are from burials that originated in the upper levels, while the age determinations on wood charcoal include seven from the lower levels and three from the upper levels. The human bone age determinations have been calibrated with mixed atmospheric and marine curves, using the percentage marine diet obtained by isotope analysis (Conte and Molle 2014, 129). The wood charcoal age determinations are evenly divided between

Table 8: Age determinations for Hane site

θ	Context	Laboratory	CRA	Material	Reference
27	Lower	Beta-260937	1070 \pm 40	cf. palm wood charcoal	Conte and Molle (2014, 129)
28	Lower	Wk-29718	1088 \pm 25	unidentified charcoal	Conte and Molle (2014, 129)
29	Lower	Wk-27331	928 \pm 30	unidentified charcoal	Conte and Molle (2014, 129)
30	Lower	Beta-260938	810 \pm 40	twig charcoal	Conte and Molle (2014, 129)
31	Lower	Beta-260935	1030 \pm 40	cf. palm steles charcoal	Conte and Molle (2014, 129)
32	Lower	Beta-260936	1000 \pm 40	cf. palm steles charcoal	Conte and Molle (2014, 129)
33	Lower	Beta-260934	790 \pm 40	twig charcoal	Conte and Molle (2014, 129)
34	Upper	Wk-29717	852 \pm 25	unidentified charcoal	Conte and Molle (2014, 129)
35	Upper	Wk-29716	682 \pm 25	nutshell charcoal	Conte and Molle (2014, 129)
36	Upper	Wk-27330	633 \pm 30	unidentified charcoal	Conte and Molle (2014, 129)
46	Lower	Gak-529	1100 \pm 100	unidentified charcoal	Anderson and Sinoto (2002, 250)
47	Lower	Gak-530	840 \pm 110	unidentified charcoal	Anderson and Sinoto (2002, 250)
48	Lower	Gak-531	715 \pm 100	unidentified charcoal	Anderson and Sinoto (2002, 250)
49	Lower	Gak-930	530 \pm 80	unidentified charcoal	Anderson and Sinoto (2002, 250)
50	Lower	Gak-931	660 \pm 80	unidentified charcoal	Anderson and Sinoto (2002, 250)
51	Lower	Gak-934	380 \pm 150	unidentified charcoal	Anderson and Sinoto (2002, 250)
52	Lower	WSU-490	1345 \pm 195	unidentified charcoal	Anderson and Sinoto (2002, 250)
53	Lower	WSU-516	1915 \pm 200	marine shell	Anderson and Sinoto (2002, 250)
54	Lower	P-1123	657 \pm 66	unidentified charcoal	Anderson and Sinoto (2002, 250)
55	Lower	Wk-8590	640 \pm 130	unidentified charcoal	Anderson and Sinoto (2002, 250)
56	Lower	Wk-8591	1030 \pm 150	unidentified charcoal	Anderson and Sinoto (2002, 250)
57	Lower	Wk-8592	690 \pm 60	unidentified charcoal	Anderson and Sinoto (2002, 250)
58	Upper	Wk-8593	1120 \pm 60	pearl shell	Anderson and Sinoto (2002, 250)
59	Lower	Wk-8594	1340 \pm 50	pearl shell	Anderson and Sinoto (2002, 250)
60	Lower	Wk-8595	1240 \pm 50	<i>Cassis</i> shell	Anderson and Sinoto (2002, 250)
61	Lower	Wk-8596	1230 \pm 50	<i>Cassis</i> shell	Anderson and Sinoto (2002, 250)
62	Lower	ANU-11376	1210 \pm 60	pearl shell	Anderson and Sinoto (2002, 250)
63	Upper	ANU-11384	290 \pm 60	unidentified charcoal	Anderson and Sinoto (2002, 250)
64	Lower	ANU-11385	970 \pm 60	unidentified charcoal	Anderson and Sinoto (2002, 250)
100	Lower	WSU-491	1675 \pm 195	unidentified charcoal	Anderson and Sinoto (2002, 250)
101	Lower	WSU-492	1380 \pm 160	unidentified charcoal	Anderson and Sinoto (2002, 250)
102	Lower	WSU-512	1210 \pm 195	marine shell	Anderson and Sinoto (2002, 250)
103	Lower	WSU-524	1750 \pm 140	marine shell	Anderson and Sinoto (2002, 250)
104	Lower	WSU-525	645 \pm 370	turtleshell etc.	Anderson and Sinoto (2002, 250)
105	Upper	Wk-34066	686 \pm 25	human bone	Conte and Molle (2014, 129)
106	Upper	Wk-27329	579 \pm 30	human bone	Conte and Molle (2014, 129)
107	Upper	Wk-29721	585 \pm 30	human bone	Conte and Molle (2014, 129)
108	Upper	Wk-34068	635 \pm 25	human bone	Conte and Molle (2014, 129)
109	Upper	Wk-34067	604 \pm 25	human bone	Conte and Molle (2014, 129)
110	Upper	Wk-27328	535 \pm 30	human bone	Conte and Molle (2014, 129)
111	Upper	Wk-34069	618 \pm 25	human bone	Conte and Molle (2014, 129)

materials classified as short-lived and those with a potential for in-built age. There are four age determinations on unidentified charcoal, including θ_{28} , θ_{29} , θ_{34} , and θ_{36} , and one on tentatively identified palm wood, θ_{27} , that have been classified as having potential for in-built age, and two on twigs, including θ_{30} and θ_{33} , two on tentatively identified palm steles, θ_{31} and θ_{32} , and one on a nutshell, θ_{35} , that have been classified as short-lived. The two age determinations on tentatively identified palm steles are both relatively old and they play a large role in dating the early history of the site.

Following Anderson and Sinoto (2002), a two phase chronological model was constructed, with an Upper phase corresponding to the upper levels and a Lower phase corresponding to the lower levels. The two-phase Hane model can be specified in an algebraic form that also includes the floating parameter, AD 1950, for technical reasons specific to OxCal (eq. 5).

$$\alpha_{\text{Lower}} > \Theta_{\text{Lower}} > \beta_{\text{Lower}} \geq \alpha_{\text{Upper}} > \Theta_{\text{Upper}} > \beta_{\text{Upper}} \geq 1950, \quad (5)$$

where

$$\Theta_{\text{Lower}} = (\theta_{27}, \theta_{28}, \theta_{29}, \theta_{30}, \theta_{31}, \theta_{32}, \theta_{33}, \theta_{46}, \theta_{47}, \theta_{48}, \theta_{49}, \theta_{50}, \theta_{51}, \theta_{52}, \theta_{53}, \theta_{54}, \theta_{55}, \theta_{56}, \theta_{57}, \theta_{59}, \theta_{60}, \theta_{61}, \theta_{62}, \theta_{64}, \theta_{100}, \theta_{101}, \theta_{102}, \theta_{103}, \theta_{104}) \quad (6)$$

and

$$\Theta_{\text{Upper}} = (\theta_{34}, \theta_{35}, \theta_{36}, \theta_{58}, \theta_{63}, \theta_{105}, \theta_{106}, \theta_{107}, \theta_{108}, \theta_{109}, \theta_{110}, \theta_{111}). \quad (7)$$

2.2.1 Outliers and Replicability of Hane Solutions

The three chronological solutions for Hane each identify the same seven outlier age determinations (table 9), six of which are from the Lower layers and one, θ_{34} , from the Upper layers. Four of the outlier age determinations were processed by the Washington State University (WSU) laboratory, two were processed by Gakushūin (Gak), and one by Waikato (Wk). The four outlier age determinations processed by WSU are all too old for their lower layer context, given the data and model. The two outlier age determinations processed by Gak are too young for their contexts and appear to be intrusive. The single outlier determination processed by Wk on unidentified wood charcoal is too old for its context and might either be a piece of old wood or residual in the Upper layers.

Hane Heaton Set Solution Various measures of boundary estimates for Hane (table 10) vary by eleven or fewer years over five calibrations that use the ΔR value recommended by Heaton et al. (2020). This result indicates that the calibration is replicable.

Hane Burr Set Solution Various measures of boundary estimates for Hane (table 11) mostly vary by fifteen or fewer years over five calibrations that use a ΔR estimate based on Burr et al. (2009). The exception is the credible interval for the start of Hane Lower, which varies 9–72 years. This result indicates that the calibration is replicable, but that the estimate for Hane Lower start is imprecise.

Table 9: Outliers identified by Hane chronological solutions

θ	Laboratory	Cause	Heaton	Burr	Conservative
53	WSU-516	old shell	✓	✓	✓
103	WSU-524	old shell	✓	✓	✓
49	Gak-930	intrusive	✓	✓	✓
51	Gak-934	intrusive	✓	✓	✓
100	WSU-491	old wood	✓	✓	✓
101	WSU-492	old wood	✓	✓	✓
34	Wk-29717	old wood/residual	✓	✓	✓

Table 10: Replicability of Heaton set Hane site chronology solutions

	mean	q1	median	q3	ci.inf	ci.sup
Hane Lower start	5	2	2	4	11	11
Hane Lower end	1	1	1	0	0	0
Hane Upper start	1	1	0	1	2	1
Hane Upper end	5	4	5	6	2	9

Table 11: Replicability of Burr set Hane site chronology solutions

	mean	q1	median	q3	ci.inf	ci.sup
Hane Lower start	15	3	4	10	9	72
Hane Lower end	2	2	2	1	1	1
Hane Upper start	1	2	1	1	2	0
Hane Upper end	3	4	3	2	5	2

Hane Conservative Set Solution Various measures of boundary estimates for Hane (table 12) vary by fifteen or fewer years over five calibrations that use a ΔR estimate based on Burr et al. (2009) incorporating a conservative estimate of the error. The exception is the credible interval for the start of Hane Lower, which varies 11–73 years. This result indicates that the calibration is replicable, but that the estimate for Hane Lower start is imprecise.

Table 12: Replicability of Conservative set Hane site chronology solutions

	mean	q1	median	q3	ci.inf	ci.sup
Hane Lower start	15	2	4	10	11	73
Hane Lower end	2	2	2	1	3	1
Hane Upper start	2	2	1	1	3	1
Hane Upper end	9	8	10	10	4	11

2.2.2 Hane Site Chronology

The value of ΔR has greatest influence on estimates of the end boundary for Hane Upper, where it introduces variability up to 21 years (table 13). The other three phase boundaries show less of an effect, with estimates that are typically a decade or less. In this situation, any one of the three calibration sets might be used to summarize site chronology.

Table 13: Variability in Hane site chronology solutions

	mean	q1	median	q3	ci.inf	ci.sup
Hane Lower start	3	1	1	2	7	10
Hane Lower end	1	0	0	1	1	1
Hane Upper start	1	1	1	0	1	0
Hane Upper end	19	22	21	20	19	21

The Conservative set solution is chosen to estimate Hane site chronology (table 14, fig. 6). The 95% credible interval for site establishment is AD 931–1114, given the model and data. The imprecision of this estimate is influenced by the lack of dating information from pre-settlement deposits and by inclusion of legacy dates from the Lower deposit that did not fully control for the effects of in-built age. Further analysis of confidently identified short-lived specimens from the earliest deposits of the well-controlled 2009 Hane excavation would likely increase the precision of the estimate for site establishment. The Lower deposits end in AD 1311–1384 and are succeeded by the Upper deposits, which were laid down between AD 1332–1395 and AD 1506–1691.

2.3 Hakaea Beach Site, Nuku Hiva Island

A three phase sequence was excavated at the Hakaea Beach Site (Allen and McAlister 2010). Three cultural deposits, identified as Layers VII, V, and III, are separated from one

Table 14: Summary statistics for Hane site chronology solution

	mean	sd	min	q1	median	q3	max	ci.inf	ci.sup
Hane Lower start	1002	45	881	977	995	1014	1147	931	1114
Hane Lower end	1348	20	1271	1334	1349	1364	1417	1311	1384
Hane Upper start	1368	17	1291	1358	1372	1381	1435	1332	1395
Hane Upper end	1598	51	1491	1559	1594	1631	1904	1506	1691

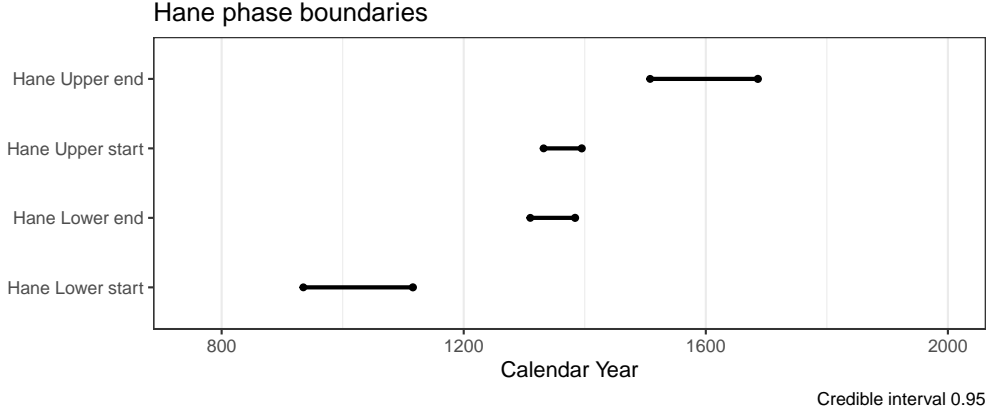


Figure 6: Hane phase boundaries, Conservative set.

another by light-colored sand deposits with limited evidence for cultural activity. Layers VI and IV each represent elapsed time between the cultural deposition evident in the layers above and below them. The Hakaea chronological model establishes boundaries between the cultural deposits such that the lower boundary is older than, or the same age as, the upper boundary to provide for the possibility that the light-colored sand deposits with limited evidence for cultural activity represent time intervals with measurable duration (eq. 8).

$$\alpha_{VII} > \Theta_{VII} > \beta_{VII} \geq \alpha_V > \Theta_V > \beta_V \geq \alpha_{III} > \theta_{38} > \beta_{III} > 1950, \quad (8)$$

where

$$\Theta_{VII} = (\theta_{22}, \theta_{23}, \theta_{24}, \theta_{37}) \quad (9)$$

and

$$\Theta_V = (\theta_{39}, \theta_{40}, \theta_{41}). \quad (10)$$

The Hakaea dating program took care to date mostly identified short-lived charcoal. Ten age determinations have been reported (Allen and McAlister 2010, 59), including four from Layer VII, three from Layer V, and one from Layer III (table 15). Two age determinations from isolated features are not assigned a position in the site stratigraphic sequence and are not included in this analysis.

Most of the age determinations are on carbonized coconut nutshell, which has negligible in-built age and can be classified as short lived. In addition, θ_{41} is a sample identified as a monocot stem characterized as a short-lived material (Allen and McAlister 2010, 58). The age determination for θ_{37} on a piece of charcoal from a tree with a known life span of 80–90 years (Allen and McAlister 2010, 58) exhibits potential for in-built age.

Table 15: Age determinations for Hakaea Beach, Nuku Hiva

θ	Context	Laboratory	CRA	Material	Reference
22	VII	Wk-22226	744 ± 30	<i>C. nucifera</i> endocarp charcoal	Allen and McAlister (2010)
23	VII	Wk-22228	746 ± 30	<i>C. nucifera</i> endocarp charcoal	Allen and McAlister (2010)
24	VII	Wk-22227	824 ± 30	<i>C. nucifera</i> endocarp	Allen and McAlister (2010)
37	VII	Wk-19934	744 ± 33	<i>B. asiatica</i> charcoal	Allen and McAlister (2010)
38	III	OZM070	535 ± 35	cf. coconut endocarp, charcoal	Allen and McAlister (2010)
39	V	OZM073	615 ± 35	coconut endocarp charcoal	Allen and McAlister (2010)
40	V	OZM071	600 ± 40	cf. coconut endocarp charcoal	Allen and McAlister (2010)
41	V	OZM072	670 ± 40	monocot stem	Allen and McAlister (2010)

2.3.1 Outliers and Replicability of Hakaea Beach Solutions

Chronological solutions for the Hakaea Beach site did not identify outliers.

Hakaea Beach Heaton Set Solution Various measures of boundary estimates for Hakaea Beach (table 16) mostly vary by seven or fewer years over five calibrations that use the ΔR value recommended by Heaton et al. (2020). The exceptions are the credible intervals for Hakaea VII start, which vary by more than 50 years. This result indicates that the calibration is replicable, but that the estimate for Hakaea VII start is imprecise.

Table 16: Replicability of Heaton set Hakaea site chronology solutions

	mean	q1	median	q3	ci.inf	ci.sup
Hakaea VII start	1	1	0	0	51	76
Hakaea VII end	1	0	0	1	3	7
Hakaea V start	0	0	0	2	1	1
Hakaea V end	1	0	1	0	2	2
Hakaea III start	0	1	0	1	2	1
Hakaea III end	1	0	1	1	3	7

Hakaea Beach Burr Set Solution Various measures of boundary estimates for Hakaea Beach (table 16) mostly vary by six or fewer years over five calibrations that use a ΔR estimate based on Burr et al. (2009). The exceptions are the credible intervals for Hakaea VII start, which vary by 64–83 years, the upper credible interval for Hakaea VII end, which varies 50 years, and the upper credible interval for Hakaea III end, which varies 18 years. This result indicates that the calibration is replicable.

Table 17: Replicability of Burr set Hakaea Beach site chronology solutions

	mean	q1	median	q3	ci.inf	ci.sup
Hakaea VII start	5	1	0	0	64	83
Hakaea VII end	5	1	1	4	2	50
Hakaea V start	3	1	2	6	2	2
Hakaea V end	3	1	3	3	1	1
Hakaea III start	2	2	1	1	6	1
Hakaea III end	3	1	1	1	4	18

Hakaea Beach Conservative Set Solution Various measures of boundary estimates for Hakaea Beach (table 18) mostly vary by eight or fewer years over five calibrations that use a ΔR estimate based on Burr et al. (2009) incorporating a conservative estimate of the error. The exceptions are the upper 95% credible interval for the end of Hakaea III, which varies by 32 years, and the confidence intervals for Hakaea VII start, which vary 63–72 years. This result indicates that the calibration is replicable.

Table 18: Replicability of Conservative set Hakaea Beach site chronology solutions

	mean	q1	median	q3	ci.inf	ci.sup
Hakaea VII start	3	2	0	1	63	72
Hakaea VII end	1	0	0	1	2	5
Hakaea V start	1	0	0	4	0	1
Hakaea V end	1	1	2	1	1	1
Hakaea III start	1	2	1	0	8	2
Hakaea III end	0	0	1	2	3	32

2.3.2 Hakaea Beach Site Chronology

The value of ΔR has no appreciable effect on estimates for most parameters (table 19), with the exception of the 95% credible intervals for Hakaea VII start, which varies by as much as 71 years. In this situation, any one of the three solutions might be used to summarize the Hakaea Beach site chronology.

Table 19: Variability in Hakaea Beach site chronology solutions

	mean	q1	median	q3	ci.inf	ci.sup
Hakaea VII start	1	1	0	1	53	71
Hakaea VII end	0	0	0	0	1	2
Hakaea V start	0	0	0	1	0	1
Hakaea V end	0	0	0	0	1	1
Hakaea III start	0	1	0	0	3	1
Hakaea III end	1	0	0	0	2	1

The Conservative set solution is chosen to estimate Hakaea Beach site chronology (table 20, fig. 7). The 95% credible interval for site establishment is AD 1174–1304; the

basal Hakaea VII deposit ends in AD 1277–1372. It is followed by Hakaea V, which starts in AD 1297–1398 and ends in AD 1325–1420, and Hakaea III, which starts in AD 1348–1447 and ends in AD 1394–1545.

Table 20: Summary statistics for Hakaea Beach site chronology solution

	mean	sd	min	q1	median	q3	max	ci.inf	ci.sup
Hakaea VII start	1272	28	944	1262	1273	1281	1383	1174	1304
Hakaea VII end	1303	22	1233	1290	1297	1308	1407	1277	1372
Hakaea V start	1337	29	1263	1318	1329	1346	1427	1297	1398
Hakaea V end	1369	30	1299	1344	1360	1398	1521	1325	1420
Hakaea III start	1406	26	1308	1392	1410	1424	1614	1348	1447
Hakaea III end	1448	42	1331	1426	1441	1459	1951	1394	1545

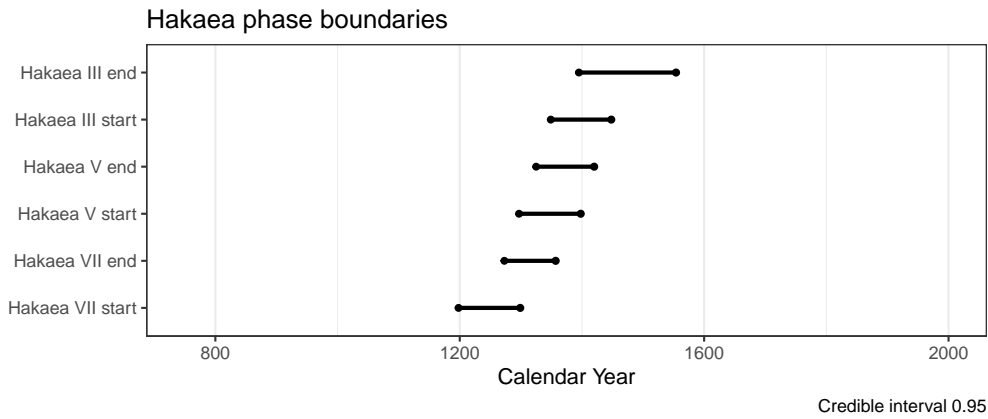


Figure 7: Hakaea phase boundaries, Conservative set.

2.4 Teavau’ua Coastal Flat, Nuku Hiva Island

Excavations at Teavau’ua on the coastal flat of Anaho Valley exposed a six layer sequence where the top three layers— Layers I, II, and IIIa—yielded historic-era artifacts and the two layers beneath them—Layers IIIb and IV—yielded traditional Marquesan artifacts (M. S. Allen 2004, 161). Layer V, the deepest deposit, is culturally sterile. There is a hiatus between Layer IV and Layer IIIb (Petchey et al. 2009, 2236). The chronological model for Teavau’ua Coastal Flat incorporates this prior chronological information by specifying the possibility of a hiatus between Layers IIIb and IV and restricting the end of Layer IIIb to radiocarbon time (eq. 11).

$$\alpha_{IV} > \Theta_{IV} > \beta_{IV} \geq \alpha_{IIIb} > \Theta_{IIIb} > \beta_{IIIb} \geq 1950, \quad (11)$$

where

$$\Theta_{IV} = (\theta_{18}, \theta_{19}, \theta_{20}, \theta_{42}, \theta_{43}, \theta_{44}, \theta_{45}, \theta_{88}) \quad (12)$$

and

$$\Theta_{\text{IIIb}} = (\theta_{89}, \theta_{90}, \theta_{91}, \theta_{92}, \theta_{98}, \theta_{99}). \quad (13)$$

Fourteen ^{14}C age determinations from Teavau'ua have been reported in the literature, eight from Layer IV and six from Layer IIIb (table 21). Eight of the age determinations have potential in-built age, including three on unidentified wood charcoal from Layer IV and three on unidentified wood charcoal and two on long-lived trees from Layer IIIb. Five age determinations from Layer IV are classified as short-lived, including three on nutshell charcoal and two on the marine shells *Periglypta reticulata* and *Pinctada margaritifera*. A single age determination on the marine shell *Periglypta reticulata* from Layer IIIb is classified as short-lived.

Table 21: Age determinations for Teavau'ua Coastal Flat site

θ	Context	Laboratory	CRA	Material	Reference
18	IV	Wk-20134	696 \pm 31	cf. <i>C. nucifera</i> nutshell charcoal	Petchey et al. (2009, 2240)
19	IV	OZI-974	730 \pm 40	nutshell charcoal	Petchey et al. (2009, 2240)
20	IV	Wk-20135	751 \pm 31	cf. <i>C. nucifera</i> nutshell charcoal	Petchey et al. (2009, 2240)
42	IV	Wk-13833	1169 \pm 36	<i>P. margaritifera</i> shell	Petchey et al. (2009, 2240)
43	IV	Wk-20133	1172 \pm 30	<i>P. reticulata</i> shell	Petchey et al. (2009, 2240)
44	IV	OZI-975	805 \pm 40	unidentified wood charcoal	M. S. Allen (2014, 6)
45	IV	OZI-976	835 \pm 45	unidentified wood charcoal	M. S. Allen (2014, 6)
88	IV	Wk-10644	635 \pm 61	unidentified wood charcoal	M. S. Allen (2004, 161)
89	IIIb	Beta-108023	430 \pm 80	unidentified wood charcoal	M. S. Allen (2004, 161)
90	IIIb	Wk-10844	395 \pm 82	unidentified wood charcoal	M. S. Allen (2004, 161)
91	IIIb	Wk-10645	379 \pm 57	unidentified wood charcoal	M. S. Allen (2004, 161)
92	IIIb	Wk-10843	341 \pm 50	cf. <i>Tournefortia</i> charcoal	M. S. Allen (2004, 161)
98	IIIb	Wk-20132	710 \pm 37	<i>P. reticulata</i> shell	Petchey et al. (2009, 2240)
99	IIIb	Wk-19116	296 \pm 34	<i>T. populnea</i> wood charcoal	Petchey et al. (2009, 2240)

2.4.1 Outliers and Replicability of Teavau'ua Solutions

The Teavau'ua chronological solutions did not identify outliers.

Teavau'ua Heaton Set Solution Various measures of boundary estimates for Teavau'ua (table 22) vary by eleven or fewer years over five calibrations that use the ΔR value recommended by Heaton et al. (2020). This result indicates that the calibration is replicable.

Table 22: Replicability of Heaton set Teavau'ua site chronology solutions

	mean	q1	median	q3	ci.inf	ci.sup
Teavauua IV start	4	2	2	4	4	2
Teavauua IV end	0	2	0	1	1	2
Teavauua IIIb start	1	2	1	0	2	2
Teavauua IIIb end	5	6	3	5	5	11

Teavau'ua Burr Set Solution Various measures of boundary estimates for Teavau'ua (table 23) vary by nine or fewer years over five calibrations that use a ΔR estimate based on Burr et al. (2009). This result indicates that the calibration is replicable.

Table 23: Replicability of Burr set Teavau'ua site chronology solutions

	mean	q1	median	q3	ci.inf	ci.sup
Teavauua IV start	4	1	1	4	4	3
Teavauua IV end	1	2	1	1	2	2
Teavauua IIIb start	1	1	1	1	1	1
Teavauua IIIb end	3	4	2	3	2	9

Teavau'ua Conservative Set Solution Various measures of boundary estimates for Teavau'ua (table 24) vary by twelve or fewer years over five calibrations that use a ΔR estimate based on Burr et al. (2009) incorporating a conservative estimate of the error. This result indicates that the calibration is replicable.

Table 24: Replicability of Conservative set Teavau'ua site chronology solutions

	mean	q1	median	q3	ci.inf	ci.sup
Teavauua IV start	1	0	1	1	3	1
Teavauua IV end	0	1	0	1	2	1
Teavauua IIIb start	1	2	1	2	3	2
Teavauua IIIb end	5	8	3	5	6	12

2.4.2 Teavau'ua Site Chronology

The value of ΔR has relatively little effect on the chronology of the Teavau'ua site (table 25). Most estimates vary by less than five years, and the maximum is 11 years. In this situation any one of the three solutions might be used to summarize Teavau'ua site chronology.

Table 25: Variability in Teavau'ua site chronology solutions

	mean	q1	median	q3	ci.inf	ci.sup
Teavauua IV start	2	1	1	2	4	2
Teavauua IV end	0	1	0	1	1	2
Teavauua IIIb start	1	2	1	1	3	1
Teavauua IIIb end	4	4	2	4	4	11

The Conservative set solution was selected (table 26, fig. 8). The 95% credible interval for site establishment is AD 1189–1377. The basal deposit, Teavauua IV, ends in AD 1291–1448. It is followed by Teavauua IIIb, which starts in AD 1413–1637 and ends in AD 1519–1823.

Table 26: Summary statistics for Teavau'ua site chronology solution

	mean	sd	min	q1	median	q3	max	ci.inf	ci.sup
Teavauua IV start	1265	52	1006	1235	1259	1279	1384	1189	1377
Teavauua IV end	1372	43	1275	1338	1376	1397	1622	1291	1448
Teavauua IIIb start	1521	60	1297	1481	1523	1563	1662	1413	1637
Teavauua IIIb end	1661	80	1502	1602	1652	1699	1951	1519	1823

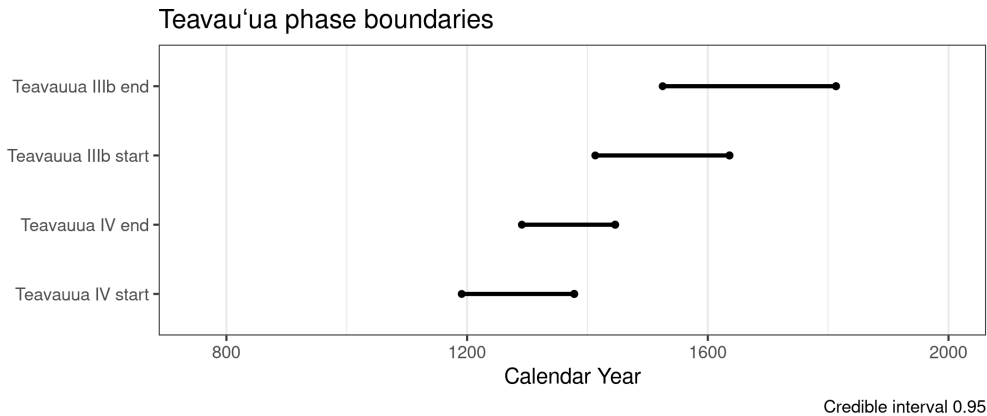


Figure 8: Teavau'ua phase boundaries, Conservative set.

2.5 Ho'oumi, Nuku Hiva Island

Ho'oumi is a deep, narrow valley with a permanent stream, located adjacent to Taipivai, one of the largest valleys on Nuku Hiva. It has a well-protected bay. The Ho'oumi site was discovered and investigated in 1956–1957 by Suggs (1961) during field work that also included excavations at Ha'atuatua. It is located close to the beach on a coastal flat adjacent to the river bank. In an area with large *paepae* (house platforms) on the ground surface, Suggs opened five pits with a combined area of around 72 m². He identified two cultural deposits separated by a layer of sterile sand in a stratigraphic sequence extending about 75 cm from the surface. In the deepest deposit, excavations revealed pavements made of stone slabs, which Suggs identified as Paved *Paepae*. The artifacts include a single ceramic sherd, around 50 pearl shell one-piece fishhooks considered by Suggs to be chronologically diagnostic, five trolling lure points and 39 coral files, in addition to cowrie-shell peelers, poi pounders, adzes and ornaments. A large majority of the fishhooks consist of ones with straight shanks, which Suggs identified as “jabbing” and “open jabbing” forms. Suggs' work yielded limited chronological information. On the basis of his artifact seriations, but no ¹⁴C dates, Suggs (1961) proposed that the upper Ho'oumi occupation represents his Classic Period and the lower occupation represents late stages of his Developmental Period. Recent artifact studies suggest that the dominance of straight-shank one-piece fishhooks, and the absence of ones with curved or angular shanks, dates both Ho'oumi occupations to after AD 1450 (Rolett 1998,

159–175).

A reinvestigation of the Ho’oumi site in 2011 had the initial goal of locating Suggs’ excavation area but fieldwork was constrained by restrictions imposed by landowners and complicated by bulldozer disturbance linked with development of a beach park (Allen et al. 2021). A series of four trenches was opened using a backhoe, in addition to excavation of a 1 m² test pit, all estimated to lie about 20–50 m seaward of Suggs’ excavation area. Sediments from the trenches were not screened; selected sediments from the 1 m² test pit were screened using 3.2 mm mesh, with the remainder processed with 6.3 mm mesh due to time constraints (Allen et al. 2021, 79). In these circumstances, artifacts and faunal remains removed during excavation have a lower probability of being identified and collected than if the excavations had been carried out under more controlled conditions. It is not a criticism of the reinvestigation of the Ho’oumi site to note that the apparent paucity of artifacts and faunal remains might be due, in part, to the excavation and collection techniques used during the limited reinvestigation in 2011, in combination with the artifact-poor nature of the exposed cultural deposits, which were identified by hearths and earth ovens visible in the trench profiles.

The 2011 reinvestigation team created three trench-specific chronological models, one for Trench 1 and two for Trench 4. Their two-phase model for Trench 1 is based on the notion that the upper boundary of Layer IV, coincident with the water table as it was observed during field work, marks a turning point in the local depositional regime. A single age determination on a *Pandanus* fruit key, Wk-50155, is assigned to the Layer III deposit above the water table. Eight age determinations are assigned to Layer IV, the deposit below the water table. The chronological model does not include two Beta Analytic age determinations from Layer IV that are described as “range finder samples” (Allen, Lewis, and Porch 2022, 9). In both cases, the Beta Analytic age determinations are younger than the single age determination from the Layer III deposit above the water table, which was “intended as a constraint” (Allen, Lewis, and Porch 2022, 9) on the age determinations from Layer IV below the water table. The excavators also constructed two two-phase chronological models for Trench 4. Their preferred model uses a ΔR value of -262 ± 28 for Phase B, and a ΔR value of -136 ± 65 for Phase D. Nevertheless, as discussed in the Introduction, we consider both of these ΔR values to be problematic. The results of this model are not discussed further here. The other chronological model uses a ΔR value of -20 ± 39 and yields results for Trench 4 (Allen et al. 2021, Table 5) that fit comfortably with the results of the site-wide chronological model developed here (see table 33), which is based on a stratigraphic interpretation that differs from the interpretation preferred by the excavators. The following sections describe these differences and their motivation in detail.

The 2011 Reinvestigation: Stratigraphy Given the close connection between stratigraphic interpretation and the chronological model used as prior information in a Bayesian calibration (Dye and Buck 2015), chronological models proposed by the 2011 reinvestigation

team must be considered in light of the site stratigraphy. In each of the four trenches excavated in 2011, the exposed stratigraphy includes a surface cultural deposit extending to depths of around 50 cm and identified as either Layer I, the upper in situ cultural occupation, or as a “near surface cultural layer” (Allen et al. 2021, 11). This cultural deposit, which revealed a few artifacts and “six in situ features” (Allen et al. 2021, 83), is underlain in each of the trenches by Layer II, a “largely acultural sand unit” (Allen et al. 2021, 83) interpreted by the excavators as a deposit left behind by a paleotsunami. In Trench 3, the lower part of the Layer II paleotsunami deposit includes water-rounded basalt pebbles and oyster shells (Allen et al. 2021, 83). In Trench 4, the Layer II paleotsunami deposit rests on a “5–10 cm thick layer of densely packed basalt pebbles and coral gravel” (Allen et al. 2021, 83). The excavators identify this deposit of basalt pebbles and coral gravel as Layer IIIa or Feature 9 (Allen et al. 2021, Table 1).

Layer IIIa/Feature 9 is interpreted as the “lower cultural layer” (Allen et al. 2021, 83). Despite noted uncertainties, the excavators suggest that their sequence of “upper” and “lower” cultural layers is “most likely coeval” (Allen et al. 2021, 95) with the “upper” and “lower” cultural occupations identified by Suggs (1961). They also suggest that Layer IIIa/Feature 9, the pebble-gravel deposit, represents a cultural feature—a “simple pavement of the kind locally referred to as *ki’iki’i*” (Allen et al. 2021, 83). No cultural material was found in association with the pebble-gravel deposit; the authors suggest that “any associated deposit was removed by the marine inundation event [paleotsunami] that deposited Layer II” (Allen et al. 2021, 83). The interface of the Layer IIIa/Feature 9 pebble-gravel deposit with the overlying Layer II paleotsunami deposit is described as “very abrupt, planar” (Allen et al. 2021, 83). A basin-shaped hearth identified as Feature 1, about 10–15 cm deep and with a radius of ca. 50 cm (Allen et al. 2021, Table 1), was found immediately beneath the pebble-gravel deposit. Four short-lived material samples collected at 105 cm below surface from the hearth feature are central to the Ho’oumi site chronology. The pebble-gravel deposit lies directly above a “culturally sterile” (Allen et al. 2021, 83) deposit identified as Layer IIIb composed primarily of marine sand, but which also contains fine charcoal. Directly below Layer IIIb is another culturally sterile deposit, Layer IV, which consists of coral gravel and pebbles resting upon a coral basement formation (Allen et al. 2021, Table 2).

In Trenches 1–3, where the pebble-gravel deposit is absent, sandy culturally-sterile deposits lie directly below the paleotsunami deposit. Trench 1 is unusual in that the sandy deposits extend beneath the water table, which was observed at about 160 cm below the ground surface during excavation. Allen et al. (2021, 80) identified the stratigraphic break between Layer III and Layer IV coincident with the water table as it was observed during excavation. The excavators’ criteria for distinguishing these layers include color, texture, and structure (Allen, Lewis, and Porch 2022, Table 1). Age determinations on samples collected from Layers III and IV in Trench 1 are also central to the Ho’oumi site chronology. Sediments in Layers III and IV were interpreted to derive mainly from fluvial depositional environments (Allen, Lewis, and Porch 2022, Table 1). As explained below,

fluvial deposition has important implications for modeling the Ho’oumi chronology.

Evaluation of the Trench-Specific Chronological Models Results of the chronological models are influenced by interpretations of the Ho’oumi site stratigraphy. As such, we draw attention to two areas where, in our view, it is important to consider alternate interpretations of the Ho’oumi stratigraphy. These alternate interpretations lead to the construction of a site-wide Ho’oumi chronological model (Section 2.5.1). First, we draw attention to the Layer IIIa/Feature 9 pebble-gravel deposit in Trench 4, which is plausibly interpreted by the excavators as a “simple house pavement, similar to those known from elsewhere in Polynesia” (Allen et al. 2021, 89). The only cultural remains associated with the presumed house pavement are a basin-shaped hearth, Feature 1, (Allen et al. 2021, Table 1) lying “[d]irectly under the pebble–gravel pavement, intruding into the otherwise culturally sterile Layer IIIb” (Allen et al. 2021, 83) and the pebbles themselves. The excavators assigned the Feature 1 hearth to the lower limit of the Layer IIIa pebble-gravel deposit (Allen et al. 2021, Table 2) and it is depicted as intrusive into Layer IIIb (Allen et al. 2021, Figure 7). Based on field observations at other Marquesan sites, such as Hanamiai, we would expect the visible presence of charcoal flecking and pieces of fragmented charcoal in a stratigraphic layer associated with a hearth such as Feature 1, which had a radius of ca. 50 cm and a 10-15 cm thick concentration of charcoal (Allen et al. 2021, 83). This is because charcoal spreads easily, especially when hearths and earth ovens are used repeatedly. In cases where hearths were used for a limited number of burning events, it is not unusual to find multiple, similar features that may have been used for everyday activities. Thus, the lack of charcoal in Layer IIIa suggests to us that even though the upper surface of the Feature 1 pit abuts the lower interface of Layer IIIa, Feature 1 was not cut from Layer IIIa. If so, then Feature 1 predates Layer IIIa by an undetermined interval.

In short, although Feature 1 lies directly under the Layer IIIa pebble–gravel deposit, its stratigraphic relation to the otherwise culturally sterile Layer IIIb is not clear. We also note that artifacts and midden, which are generally dispersed throughout living floor deposits, were not recovered from Layer IIIa, and architectural features such as post holes and stone slabs were also absent. Finally, the fact that the pebbles in Layer IIIa are natural rather than worked raises the possibility that they could have been deposited without human intervention.

Taken together, the lack of unequivocal evidence for the house pavement hypothesis, including uncertainty surrounding the stratigraphic association of Feature 1, focuses attention on the potential of using alternate stratigraphic interpretations to develop chronological models for the Ho’oumi site. With this in mind, we suggest that Feature 1 represents the base of a pit that was first truncated by the paleotsunami, then buried by the deposit left behind as the inundation subsided. In this interpretation, the densely packed deposit of basalt pebbles and coral gravel comprises part of the paleotsunami deposit, rather than a house pavement. Feature 1 can be interpreted separately from the

pebble-gravel deposit. It consists of at least two units of stratification: (i) the interface created when the pit was excavated; and (ii) the deposit(s) that subsequently filled the open pit after its use. The Feature 1 fill may represent a mix of materials, including those related to its use as a fire feature and other materials from the deposit(s) from and through which the pit was cut; the latter materials may have contributed to filling the open pit after it went out of use as a fire feature.

Thus, it is suggested here that the pebble-gravel deposit in Trench 4 represents a residual deposit of coarser particles laid down as the energy of the inundation event began to dissipate. As the energy of the inundation event dissipated further, the finer particles identified as Layer II were deposited on top of the densely packed deposit of basalt pebbles and coral gravel. This interpretation fits well with the stratigraphic record for the paleotsunami deposit in Trench 3, where water-rounded basalt pebbles and oyster shells were also buried by finer particles in the upper levels. The lack of cultural material associated with the Trench 4 pebble-gravel deposit does not require a special explanation because the paleotsunami deposit as a whole, and to which the pebble-gravel deposit is interpreted to belong, is “largely acultural” (Allen et al. 2021, 83). The hypothesis that the pebble-gravel deposit comprises part of a paleotsunami deposit might be tested by grain-size analysis and characterization of the sedimentary fabric of the deposit (Paris et al. 2020) together with a controlled areal excavation adjacent to Trench 4 to search for cultural materials associated with Layer IIIa.

In summary, the excavators’ interpretation of Trench 4 fails to explain the lack of artifacts associated with the Layer IIIa deposit and it raises significant questions concerning the stratigraphic relation of Feature 1 to Layer IIIa. The alternative interpretation developed here resolves both of these problems: (i) materials deposited by a paleotsunami would include artifacts only coincidentally, so the lack of artifacts in Layer IIIa is expected; and (ii) Feature 1 was truncated by the paleotsunami, which removed evidence for the surface from which Feature 1 was cut. This different interpretation of the pebble-gravel deposit has implications for modeling the four age determinations associated with the Feature 1 hearth.

We turn now to the Trench 1 stratigraphic sequence, where the sandy deposits extend below the water table at about 160 cm below ground surface, and the waterlogged Layer IV deposit is rich in anaerobically-preserved organic materials. The trench was excavated with a mechanical digger to 250 cm below surface with a width of 50 cm. The critical portion of the stratigraphic sequence, in relation to chronological models, consists of Layers III and IV. As interpreted by the excavators, Layer IV is the deposit below the water table, and the top of the water table coincides with the interface between Layers III and IV. Both layers were deposited in a fluvial setting associated with a river that was located about 70 m from Trench 1 in 2011 (Allen, Lewis, and Porch 2022, 7). Eight of the Trench 1 age determinations are for samples of botanical material found in blocks of intact sediment collected from the deepest levels of the waterlogged Layer IV deposit. The sediment blocks represent five ca. 15 cm levels reaching from 175–250 cm below surface.

Two additional age determinations were obtained for an adzed timber provenanced to ca. 190–235 cm below surface, also from the waterlogged Layer IV deposit (Allen, Lewis, and Porph 2022, Table 2). For the above-lying Layer III, there is a single age determination on a botanical specimen.

Questions raised here focus on the coincidence of the water table and the stratigraphic boundary between Layers III and IV, which introduces a strong stratigraphic constraint on age determinations from below the water table into the excavators' chronological model (Allen, Lewis, and Porph 2022, 9). It is important to note that the Bayesian analysis interprets this boundary as certain; age determinations on materials recovered from sediments below the boundary must be older than age determinations on materials recovered from sediments above the boundary. As a consequence, the excavators remove as outliers age determinations from Layer IV that are younger than the single age determination for Layer III from the model. Can one be confident that materials recovered from Layer III are younger than those recovered from Layer IV? In our view, considerations of the fluvial mode of deposition for Layers III and IV (Allen, Lewis, and Porph 2022, Table 1) indicate that the certainty assumed by the Bayesian analysis lacks solid support in the excavators' stratigraphic interpretation. We also draw attention to uncertainty surrounding the claim that the Layer III/IV boundary marks a turning point in the local depositional regime. As a result, we propose a more conservative model, specifically one that treats Layers III and IV as a single entity.

Rivers continually pick up and drop material as they flow, so there is no basis for an assumption that materials in a fluvial deposit are sorted by age. Indeed, residual materials older than the context from which they were recovered are expected in fluvial deposits. Both the waterlogged Layer IV deposit and the dark gray Layer III deposit above it are expected to contain a mix of materials of different ages, unsorted stratigraphically. In order to be certain that materials recovered from Layer III are younger than those recovered from Layer IV, as the Bayesian model proposed by Allen, Lewis, and Porph (2022) assumes, the Layer III/IV boundary would have to represent an interval of time sufficient to offset the expected effects of residuality.

Uncertainty about recorded characteristics of the Trench 1 sediments directly above and below the Layer III/IV interface further clouds the interpretation that these two deposits represent distinct sediment facies that might be separated in time. Although the excavators claim that the stratigraphic layers in Trench 1 were "largely differentiated on colour" (Allen, Lewis, and Porph 2022, 7), the sediment descriptions appear to indicate that sediment colors in all trenches fall within a narrow range that occupies the lower left quadrant of a single hue on the Munsell color chart (Allen, Lewis, and Porph 2022, Table 1). For example, the color of presumably dry sediment from Layer IV is described as "dark grey brown" and the same color name is used to describe dry sediment from Layer III (Allen et al. 2021, 80), although the Munsell color offered in support (10YR 4/3) indicates a plain brown color instead (Allen, Lewis, and Porph 2022, Table 1). As a result, it is difficult to be confident that the sediment color data support the claim that

the Layer III/IV boundary marks a turning point in the local depositional regime.

The excavators also distinguished the Layer III sediments from those of Layer IV on the basis of “sedimentological and palaeobiological analyses” (Allen, Lewis, and Porch 2022, Table 2, note b). The sedimentological analyses include laser granulometry for Layer IV but not for Layer III, so there is no basis for a direct comparison. However, description of the Layer IV sediments as “silty sand”, and the Layer III sediments as “loamy coarse sand” (Allen, Lewis, and Porch 2022, Table 1) provides a general contrast. With respect to the palaeobiological content, the waterlogged sediments are expected to preserve the botanical and other organic materials recovered from Layer IV, while similar materials deposited in the dry sediments of Layer III would have decayed. In any case, post-depositional effects complicate the argument that the Layer III/IV boundary marks a turning point in the local depositional regime.

Do other sediment characteristics, such as structure and consistency (Allen, Lewis, and Porch 2022, Table 1), distinguish a turning point in the local depositional regime? Again, the evidence is not convincing: (i) soil structure is degraded in a waterlogged environment, so the difference between the moderate crumb structure of Layer III and the massive nature of Layer IV might well be at least partially post-depositional; and (ii) consistency was measured dry for Layer III and wet for Layer IV, so these observations are not strictly comparable. In fact, the excavators’ uncertainty about the Layer III/IV boundary appears to be indicated by its representation as a dashed line in the stratigraphic profile (Allen, Lewis, and Porch 2022, Fig. 3). The certainty expected by the Bayesian analysis is nowhere to be found.

Consequently, the interpretation adopted here does not recognize the Layer III/IV boundary as a stratigraphic or phase boundary. In so doing, this interpretation implies that differences between the characteristics of Layers III and IV, such as excellent preservation of a wide range of palaeobiological remains and dark color, are due to the waterlogged condition of Layer IV, rather than a change in the local depositional regime. Treating Layers III and IV as a single entity, as we have done in our Ho’oumi model, recognizes that materials in the deposit above the water table may be residual and older than materials deposited below the water table due to the fluvial mode of deposition.

2.5.1 Ho’oumi Model

The site-wide chronological model presented here is based on the novel stratigraphic interpretation described above. The model employs phasing proposed by the excavators for Trench 4 (Allen et al. 2021, 83):

Phase D the surface deposit in each of the trenches and in Suggs’ excavations;

Phase C the paleotsunami deposit in each of the trenches, including the densely packed basalt pebbles and coral gravel in Trench 4 and the sterile sand layer separating Sugg’s upper and lower cultural deposits (Allen, Lewis, and Porch 2022, 5);

Phase A/B all deposits stratigraphically inferior to the paleotsunami deposit in each of the trenches, including Suggs’ lower cultural deposit.

As there are no age determinations from Phase C, the site-wide model consists of two phases, Phases A/B and D. Among the age determinations for Phase A/B is a single short-lived material sample collected by Suggs from Hearth 1, which is directly associated with one of the largest stone pavements and the ceramic sherd (Allen, Dickinson, and Huebert 2012, 98). Suggs links these finds to the lower occupation: “One sherd of poorly fired pottery was found in the lower stratum associated with the Paved Paepae” (Suggs 1961, 56). Results of the site-wide two phase model can be compared to the individual trench models created by the excavators, through the method of multiple working hypotheses (Chamberlin 1965; Elliot and Brook 2007).

There are 18 ^{14}C age determinations for 15 events from Ho’oumi (table 27). Events θ_{123} , θ_{127} , and θ_{129} are each associated with two ^{14}C age determinations; material from each of the samples was analyzed separately by two different labs. In the cases of θ_{127} and θ_{129} , the age determinations supported one another and have been combined. In the case of the adzed timber, θ_{123} , the two age determinations did not support one another, nevertheless it is not clear which one is the better estimate. They were both included in the prior to see if stratigraphic constraints and associated data were sufficient to distinguish one or the other as an outlier. The results show that both age determinations fit comfortably within the site chronology, as might be expected for a fluvial deposit where materials are frequently reworked and redeposited.

The Ho’oumi age determinations have been modeled as a two phase sequence (eq. 14), with phase designations based on Allen et al. (2021, 83). Phase D, the youngest, includes age determinations from Layer I in Trench 2 and Trench 4. Phase A/B includes age determinations from Layers III, IIIa, IV, and Suggs’ lower cultural deposit.

$$\alpha_{A/B} > \Theta_{A/B} > \beta_{A/B} \geq \phi_{\text{tsunami}} \geq \alpha_D > \Theta_D > \beta_D > 1950, \quad (14)$$

where

$$\Theta_D = (\theta_{116}, \theta_{117}), \quad (15)$$

and

$$\Theta_{A/B} = (\theta_{17}, \theta_{112}, \theta_{113}, \theta_{114}, \theta_{115}, \theta_{118}, \theta_{123}, \theta_{124}, \theta_{125}, \theta_{126}, \theta_{127}, \theta_{128}, \theta_{129}). \quad (16)$$

2.5.2 Outliers and Replicability of Ho’oumi Solutions

The three chronological solutions for the Ho’oumi site each identify a single outlier, the age determination θ_{118} from Suggs’ lower cultural layer (table 28). This age determination is identified as intrusive because it post-dates the expected age of the context from which it was recovered. Based on a proposed correlation of paleotsunami deposits across the site (Allen, Lewis, and Porch 2022, 5), it is expected that the age of Suggs’ lower occupation pre-dates the paleotsunami, but this is not the case; the age determination is significantly younger.

Table 27: Age determinations for Ho'oumi site

θ	Context	Laboratory	CRA	Material	Reference
117	A/B	Beta-303442	720 \pm 30	<i>C. nucifera</i> endocarp charcoal	M. S. Allen (2014, 4)
112	A/B	Wk-51233	775 \pm 13	<i>C. nucifera</i> endocarp charcoal	Allen et al. (2021)
113	A/B	Wk-51794	798 \pm 19	carbonised fruit	Allen et al. (2021)
114	A/B	Wk-51234	1031 \pm 21	<i>P. margaritifera</i> shell	Allen et al. (2021)
115	A/B	Beta-303443	550 \pm 30	<i>C. nucifera</i> endocarp charcoal	Allen et al. (2021)
116	D	Wk-49637	811 \pm 24	<i>P. margaritifera</i> shell	Allen et al. (2021)
117	D	Wk-51238	152 \pm 23	<i>C. lupus familiaris</i> phalange	Allen et al. (2021)
118	A/B	Beta-296679	130 \pm 30	<i>A. moluccanus</i> endocarp	Allen, Dickinson, and Huebert (2012, 94)
123	A/B	Wk-50151	933 \pm 25	adzed <i>Syderoxyylon</i> timber	Allen, Lewis, and Porch (2022)
123	A/B	Beta-303441	710 \pm 30	adzed <i>Syderoxyylon</i> timber	Allen, Lewis, and Porch (2022)
124	A/B	Wk-50155	886 \pm 25	<i>Pandanus</i> fruit key	Allen, Lewis, and Porch (2022)
125	A/B	Wk-49523	928 \pm 26	<i>Pandanus</i> fruit key	Allen, Lewis, and Porch (2022)
126	A/B	Wk-50152	905 \pm 25	<i>C. nucifera</i> immature fruit	Allen, Lewis, and Porch (2022)
127	A/B	Wk-50154	930 \pm 25	<i>C. nucifera</i> immature fruit	Allen, Lewis, and Porch (2022)
127	A/B	UCIAMS-230703	975 \pm 20	<i>C. nucifera</i> immature fruit	Allen, Lewis, and Porch (2022)
128	A/B	Wk-49524	909 \pm 24	<i>C. nucifera</i> immature fruit	Allen, Lewis, and Porch (2022)
129	A/B	Wk-50153	936 \pm 25	<i>Pandanus</i> fruit key	Allen, Lewis, and Porch (2022)
129	A/B	UCIAMS-230702	955 \pm 20	<i>Pandanus</i> fruit key	Allen, Lewis, and Porch (2022)

Table 28: Outliers identified by Ho’oumi chronological solutions

θ	Laboratory	Cause	Heaton	Burr	Conservative
118	Beta-296679	intrusive	✓	✓	✓

Ho’oumi Heaton Set Solution Various measures of boundary estimates for Ho’oumi (table 29) vary by eight or fewer years over five calibrations that use the ΔR value recommended by Heaton et al. (2020). Most of the estimates vary by two years or less. This result indicates that the calibration is replicable.

Table 29: Replicability of Heaton set Ho’oumi site chronology solutions

	mean	q1	median	q3	ci.inf	ci.sup
Start Ho’oumi A/B	2	2	0	1	4	2
End Ho’oumi A/B	1	0	0	1	6	3
Paleotsunami	1	1	0	1	2	3
Start Ho’oumi D	1	1	1	1	7	8
End Ho’oumi D	2	1	3	3	1	2

Ho’oumi Burr Set Solution Various measures of boundary estimates for Ho’oumi (table 30) vary by 6 or fewer years over five calibrations that use the ΔR value based on the reservoir age established by Burr et al. (2009). This result indicates that the calibration is replicable.

Table 30: Replicability of Burr set Ho’oumi site chronology solutions

	mean	q1	median	q3	ci.inf	ci.sup
Start Ho’oumi A/B	1	3	1	0	2	2
End Ho’oumi A/B	1	1	0	1	6	5
Paleotsunami	1	1	1	1	4	2
Start Ho’oumi D	1	2	1	0	3	3
End Ho’oumi D	1	1	2	3	1	2

Ho’oumi Conservative Set Solution Various measures of boundary estimates for Ho’oumi (table 31) vary by ten or fewer years over five calibrations that use a ΔR estimate based on Burr et al. (2009) incorporating a conservative estimate of the error. Most of the estimates vary by ten years or less. This result indicates that the calibration is replicable.

2.5.3 Ho’oumi Site Chronology

The value of ΔR has a relatively small effect on the Ho’oumi chronology (table 32). All of the estimates yield results that vary by four years or less. In this situation, calibrations from any one of the sets might be used to establish site chronology.

The Conservative set solution is chosen to estimate the Ho’oumi chronology (table 33, fig. 9). The 95% credible interval for site establishment is $\text{AD } 1022\text{--}1173$; the earliest

Table 31: Replicability of Conservative set Ho’oumi site chronology solutions

	mean	q1	median	q3	ci.inf	ci.sup
Start Ho’oumi A/B	1	3	1	0	1	1
End Ho’oumi A/B	0	0	0	1	7	7
Paleotsunami	0	0	0	1	3	3
Start Ho’oumi D	1	1	1	0	9	10
End Ho’oumi D	2	1	2	3	2	2

Table 32: Variability in Ho’oumi site chronology solutions

	mean	q1	median	q3	ci.inf	ci.sup
Start Ho’oumi A/B	0	3	1	0	1	1
End Ho’oumi A/B	0	0	0	0	4	2
Paleotsunami	0	0	0	1	3	3
Start Ho’oumi D	1	1	1	0	2	3
End Ho’oumi D	1	1	2	3	1	2

phase, Ho’oumi A/B, ends in AD 1359–1552. The most recent deposit, Ho’oumi D, dates to between AD 1465–1800 and AD 1690–1932. The paleotsunami is estimated to have occurred in AD 1422–1697.

Table 33: Summary statistics for Ho’oumi site chronology solution

	mean	sd	min	q1	median	q3	max	ci.inf	ci.sup
Start Ho’oumi A/B	1115	46	628	1095	1131	1147	1199	1022	1173
End Ho’oumi A/B	1457	44	1308	1431	1452	1480	1769	1359	1552
Paleotsunami	1548	76	1309	1491	1541	1601	1910	1422	1697
Start Ho’oumi D	1640	81	1334	1589	1652	1691	1945	1465	1800
End Ho’oumi D	1786	74	1653	1724	1761	1847	1952	1690	1932

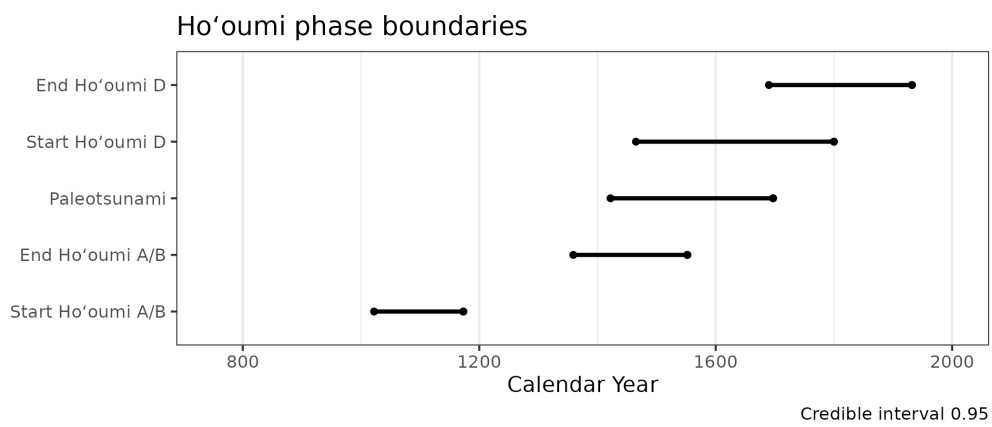


Figure 9: Ho'oumi phase boundaries and paleotsunami estimate, Conservative set.

2.6 Ha'atuatua Site, Nuku Hiva Island

The Ha'atuatua site was first investigated and dated by Suggs (1961). The site was briefly investigated by Sinoto (1966) and later re-excavated and dated by Rolett and Conte (1995). Subsequent investigations carried out by Rolett have not been published yet but the results are partially summarized here and in Supplement 3.

The Ha'atuatua site is situated within the largest dune complex in the Marquesas, a formation measuring 750 m long and extending 250 m inland. Stream channels cut through the dunes toward the north and south of the complex (Rolett and Conte 1995, 198, Fig. 2). Here, we refer to the “main dune” as the area situated between the two stream channels. Location A, the most important focus of Suggs' excavations and later research, is on the main dune near a scarp rising from the beach. The “central dune” zone, lying inland from Location A, was investigated in 1992 by Rolett and Conte through coring, test excavations and a 4 m² areal excavation. In 1994, another 4 m² areal excavation was opened about 100 m south of Location A—we refer to this location as the “southern main dune.” Our analysis of the Ha'atuatua chronology draws upon age determinations from these three areas: Location A, the central dune and the southern main dune.

Situated north of the northernmost stream, Suggs' Location B is distant from and peripheral to excavation areas on the main dune. Seven of the Ha'atuatua age determinations derive from excavations at Location B (table 34). These are excluded from our analysis because it is not yet possible to correlate the Location B strata with those of the main dune. The age determination I-394A, which is from Location A, is excluded because it is on human bone from a burial whose stratigraphic context is not secure.

Table 34: Excluded Ha'atuatua age determinations

Laboratory	CRA	Context	Material	Reference
I-394A	1270 ± 150	burial pit	bone	Suggs (1961)
I-394D	1090 ± 180	hearth	unidentified charcoal	Suggs (1961)
I-394L	1910 ± 180	hearth	unidentified charcoal	Suggs (1961)
I-17149	<190	hearth	unidentified charcoal	Rolett and Conte (1995, 205)
I-17150	390 ± 80	burnt surface	unidentified charcoal	Rolett and Conte (1995, 205)
I-17151	360 ± 140	burnt surface	unidentified charcoal	Rolett and Conte (1995, 205)
I-17159	310 ± 80	burnt surface	unidentified charcoal	Rolett and Conte (1995, 205)
I-17160	410 ± 90	hearth	unidentified charcoal	Rolett and Conte (1995, 205)

The same basic stratigraphic sequence is encountered across the main dune: (i) a surface deposit, Layer A, underlain by (ii) a rich, charcoal-stained deposit, Layer B, with numerous intact features—combustion structures, pavements, pits and postholes—indicating an intensive occupation that likely covered an area of 4,000 m² or more, and (iii) a light-colored deposit, Layer C, containing scattered charcoal flecking and isolated artifacts. Layer C transitions to the pre-Polynesian colonization dune. Crab disturbance is widespread, affecting all of the deposits, with crab tunnels clearly visible in the stratigraphic profiles. Across the main dune, the diagnostic artifacts are mainly

Archaic. There is no clear evidence for a Classic era occupation.

The 21 ^{14}C age determinations from Ha'atuatua considered in this analysis are listed in Table 35. Three of the age determinations are previously unpublished. Seventeen of the age determinations are on charcoal, three are on marine shells, and one is on the bone of a wedge-tailed shearwater seabird, *Puffinus pacificus*, discovered fully articulated in a collapsed burrow. The dated pieces of charcoal and marine shells are associated with human use of the site and can be confidently assigned to one of the two traditional Marquesan stratigraphic units identified at the site, Layers B and C. The seabird bone represents a natural deposit. The dated charcoal pieces were not identified and potentially incorporate in-built age. The marine shells and the sea-bird bone are considered short-lived.

Table 35: Age determinations for Ha'atuatua site

θ	Context	Laboratory	CRA	Material	Reference
68	D	Beta-140699	1080 ± 50	<i>P. pacificus</i> bone collagen	this paper
69	B	Beta-81346	820 ± 80	unidentified charcoal	this paper
70	B	Beta-81347	590 ± 70	unidentified charcoal	this paper
71	B	I-394D	1090 ± 180	unidentified charcoal	Suggs (1961)
72	B	I-17655	720 ± 110	unidentified charcoal	Rolett (1998, 51)
73	B	I-394L	1910 ± 180	unidentified charcoal	Suggs (1961)
74	B	I-394B	2080 ± 180	unidentified charcoal	Suggs (1961)
75	B	I-17152	570 ± 80	unidentified charcoal	Rolett and Conte (1995, 205)
76	B	I-17157	560 ± 80	unidentified charcoal	Rolett and Conte (1995, 205)
77	B	I-17158	460 ± 80	unidentified charcoal	Rolett and Conte (1995, 205)
78	C	CAMS-8664	1570 ± 90	<i>C. radiata</i> shell	Rolett and Conte (1995, 205)
79	C	CAMS-8665	960 ± 70	unidentified charcoal	Rolett and Conte (1995, 205)
80	C	CAMS-8662	1630 ± 80	marine shell	Rolett (1998, 51)
81	B	I-17657	230 ± 90	unidentified charcoal	Rolett (1998, 51)
82	C	CAMS-8663	940 ± 60	marine shell	Rolett (1998, 51)
83	B	I-17656	210 ± 90	unidentified charcoal	Rolett (1998, 51)
84	B	I-17654	500 ± 110	unidentified charcoal	Rolett (1998, 51)
85	C	CAMS-8666	490 ± 70	unidentified charcoal	Rolett (1998, 51)
86	C	CAMS-19454	940 ± 60	unidentified charcoal	Rolett (1998, 51)
87	C	CAMS-19453	540 ± 60	unidentified charcoal	Rolett (1998, 51)
93	B	Gak-874	620 ± 90	unidentified charcoal	Sinoto (1966, 303)

The Ha'atuatua chronological model includes two dated stratigraphic units, B and C, that are related to the age of the seabird bone, θ_{68} , recovered from a collapsed burrow nest (eq. 17). Seabirds were preyed upon by the early Marquesan settlers and eventually abandoned their mainland nests for locations remote from human settlements, such as offshore islets. Based on the vertebrate faunal record from the Hanamiai site, shearwaters were commonly eaten and their bones comprise a substantial component of the vertebrate faunal remains for about 200 years after initial settlement (Steadman and Rolett 1996). Site chronology solutions for the Hanamiai site indicate the period of common seabird consumption lasted for 169–228 years, after which seabird consumption is not common.

Thus, a date 169–228 years before the age of the shearwater bone from the nesting burrow was modeled as a *terminus post quem* for settlement of the Ha’atuatua site.

$$(\theta_{68} - U(169, 228)) \geq \alpha_C > \Theta_C > \beta_C \geq \alpha_B > \Theta_B > \beta_B, \quad (17)$$

where

$$\Theta_B = (\theta_{69}, \theta_{70}, \theta_{72}, \theta_{74}, \theta_{75}, \theta_{76}, \theta_{77}, \theta_{81}, \theta_{83}, \theta_{84}, \theta_{93}) \quad (18)$$

and

$$\Theta_C = (\theta_{78}, \theta_{79}, \theta_{80}, \theta_{82}, \theta_{85}, \theta_{86}, \theta_{87}). \quad (19)$$

2.6.1 Outliers and Replicability of Ha’atuatua Solutions

The three chronological solutions for Ha’atuatua identify seven outliers (table 36), which are alarming numbers given that they represent a third of the 21 age determinations from the site.

Table 36: Outliers identified by Ha’atuatua chronological solutions

θ	Laboratory	Cause	Heaton	Burr	Conservative
69	Beta-81346	old wood/residual	✓	✓	✓
74	I-394B	old wood/residual	✓	✓	✓
80	CAMS-8662	old shell	✓	✓	✓
81	I-17657	intrusive	✓	✓	✓
82	CAMS-8663	old shell	✓	✓	✓
83	I-17656	intrusive	✓	✓	✓
85	CAMS-8666	intrusive	✓	✓	✓

Ha’atuatua Heaton Set Solution Various measures of boundary estimates for Ha’atuatua (table 37) mostly vary by three or fewer years over five calibrations that use the ΔR value recommended by Heaton et al. (2020). This result indicates that the calibration is replicable.

Table 37: Replicability of Heaton set Ha’atuatua site chronology solutions

	mean	q1	median	q3	ci.inf	ci.sup
Phase Haatuatua C start	2	2	2	1	3	3
Phase Haatuatua C end	0	0	1	1	2	1
Phase Haatuatua B start	1	1	1	1	1	0
Phase Haatuatua B end	0	0	0	0	2	2

Ha’atuatua Burr Set Solution Various measures of boundary estimates for Ha’atuatua (table 38) vary by six or fewer years over five calibrations that use a ΔR estimate based on Burr et al. (2009). This result indicates that the calibration is replicable.

Table 38: Replicability of Burr set Ha'atuatua site chronology solutions

	mean	q1	median	q3	ci.inf	ci.sup
Phase Haatuatua C start	1	1	1	1	6	2
Phase Haatuatua C end	0	1	1	1	2	2
Phase Haatuatua B start	0	1	1	1	1	1
Phase Haatuatua B end	0	0	0	0	1	2

Ha'atuatua Conservative Set Solution Various measures of boundary estimates for Ha'atuatua (table 39) vary by four or fewer years over five calibrations that use a ΔR estimate based on Burr et al. (2009) incorporating a conservative estimate of the error. This result indicates that the calibration is replicable.

Table 39: Replicability of Conservative set Ha'atuatua site chronology solutions

	mean	q1	median	q3	ci.inf	ci.sup
Phase Haatuatua C start	0	1	1	0	4	2
Phase Haatuatua C end	0	2	0	1	2	1
Phase Haatuatua B start	0	0	1	1	1	1
Phase Haatuatua B end	0	0	0	1	1	2

2.6.2 Ha'atuatua Site Chronology

The value of ΔR has little effect on the chronology of the Ha'atuatua site (table 40). Estimates vary by six or fewer years. In this situation, any one of the calibrations likely reflects the full uncertainty of the estimates.

Table 40: Variability in Ha'atuatua site chronology solutions

	mean	q1	median	q3	ci.inf	ci.sup
Phase Haatuatua C start	1	1	1	0	6	1
Phase Haatuatua C end	0	0	0	1	1	1
Phase Haatuatua B start	0	0	0	1	0	1
Phase Haatuatua B end	0	0	0	0	2	2

The Conservative set solution is selected to estimate Ha'atuatua site chronology (table 41, fig. 10). The 95% credible interval for site establishment is AD 1032–1203; the earliest phase, Ha'atuatua C, ends in AD 1336–1439. The later phase, Ha'atuatua B, starts in AD 1378–1446 and ends in AD 1397–1465.

Table 41: Summary statistics for Ha'atuatua site chronology solution

	mean	sd	min	q1	median	q3	max	ci.inf	ci.sup
Phase Haatuatua C start	1123	43	866	1099	1127	1152	1279	1032	1203
Phase Haatuatua C end	1394	29	1176	1376	1400	1415	1473	1336	1439
Phase Haatuatua B start	1412	19	1231	1402	1413	1424	1476	1378	1446
Phase Haatuatua B end	1431	20	1316	1419	1430	1441	1680	1397	1465

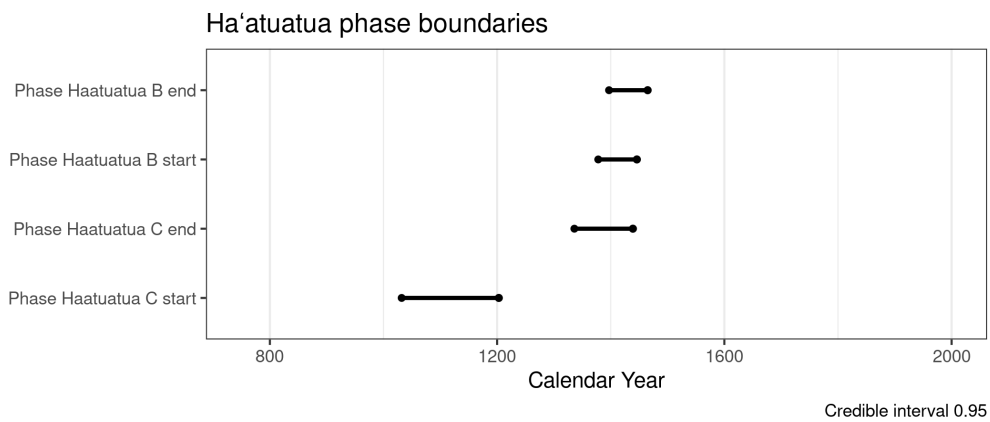


Figure 10: Ha'atuatua phase boundaries, Conservative set.

2.7 East Hanau, Hiva Oa Island

Yosihiko Sinoto excavated the East Hanau rockshelter site on Hiva Oa in the 1960's. It is one of two rockshelters on the opposing east and west coasts of Hanau Bay. Details of the excavation are not published, but a partial summary of the stratigraphy and artifact assemblages is given in Supplement 2. The excavated area of ca. 21 m² covered most of the interior of the East Hanau shelter. Sinoto identified six cultural layers. Two age determinations were obtained, one from the deepest deposit (Layer VI) and another from the upper levels (Layer II) (table 42).

Table 42: Age determinations for East Hanau site

θ	Context	Laboratory	CRA	Material	Reference
94	II	Gak-1965	320 ± 110	unidentified charcoal	Rolett (1998, 58)
95	VI	Gak-1966	930 ± 80	unidentified charcoal	Rolett (1998, 58)

The two dates are modeled according to their stratigraphic positions (eq. 20).

$$\theta_{95} > \theta_{94}. \quad (20)$$

2.7.1 Outliers and Replicability of East Hanau Solutions

The three chronological solutions for the East Hanau site did not identify outlier age determinations.

East Hanau Heaton Set Solution Various measures of boundary estimates for East Hanau (table 43) vary by five or fewer years over five calibrations that use the ΔR value recommended by Heaton et al. (2020). This result indicates that the calibration is replicable.

Table 43: Replicability of Heaton set East Hanau site chronology solutions

	mean	q1	median	q3	ci.inf	ci.sup
Gak-1966	2	1	1	2	2	2
Gak-1965	3	2	2	2	5	4

East Hanau Burr Set Solution Various measures of boundary estimates for East Hanau (table 44) vary by seven or fewer years over five calibrations that use a ΔR estimate based on Burr et al. (2009). This result indicates that the calibration is replicable.

Table 44: Replicability of Burr set East Hanau site chronology solutions

	mean	q1	median	q3	ci.inf	ci.sup
Gak-1966	1	1	1	0	5	2
Gak-1965	2	1	3	2	3	7

East Hanau Conservative Set Solution Various measures of boundary estimates for East Hanau (table 45) vary by five or fewer years over five calibrations that use a ΔR estimate based on Burr et al. (2009) incorporating a conservative estimate of the error. This result indicates that the calibration is replicable.

Table 45: Replicability of Conservative set East Hanau site chronology solutions

	mean	q1	median	q3	ci.inf	ci.sup
Gak-1966	1	2	2	1	4	1
Gak-1965	1	1	2	1	5	2

2.7.2 East Hanau Site Chronology

The value of ΔR has no appreciable effect on the East Hanau chronology (table 46), which is to be expected, given that the two age determinations from the site are both on wood charcoal. In this situation, any of the three solutions can be used to interpret site chronology.

Table 46: Variability in East Hanau site chronology solutions

	mean	q1	median	q3	ci.inf	ci.sup
Gak-1966	1	1	2	1	2	1
Gak-1965	0	0	1	1	5	3

The Conservative set solution is selected here (table 47, fig. 11). The 95% credible interval for Gak-1966 is AD 1015–1289, and for Gak-1965 is AD 1403–1810.

Table 47: Summary statistics for East Hanau site chronology solution

	mean	sd	min	q1	median	q3	max	ci.inf	ci.sup
Gak-1966	1156	81	689	1095	1164	1212	1480	1015	1289
Gak-1965	1572	108	1067	1497	1555	1636	1947	1403	1810

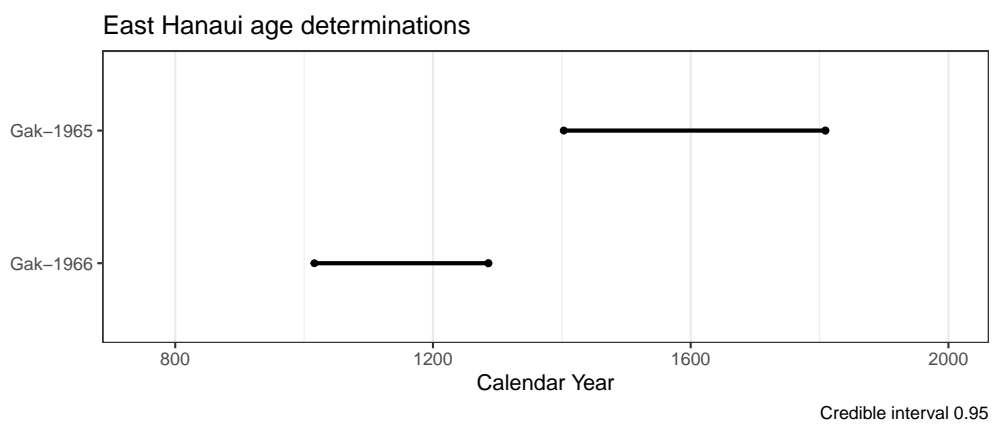


Figure 11: East Hanai age determinations, Conservative set.

2.8 West Hanauī, Hiva Oa Island

Yosihiko Sinoto excavated the West Hanauī rockshelter site on Hiva Oa in the 1960’s. It is one of two rockshelters on the opposing east and west coasts of Hanauī Bay. Details of the excavation are not published, but a partial summary of the stratigraphy and artifact assemblages is given in Supplement 2. Sinoto excavated ca. 20 m² and identified six cultural layers, with the deepest deposit (Layer VI) lying about 120 cm below surface. Two age determinations were obtained, both from Layers III or IV (table 48).

Table 48: Age determinations for West Hanauī site

θ	Context	Laboratory	CRA	Material	Reference
96	III or IV	Gak-1967	280 \pm 90	unidentified charcoal	Rolett (1998, 58)
97	III or IV	Gak-1968	440 \pm 90	unidentified charcoal	Rolett (1998, 58)

The two dates are modeled as a single phase (eq. 21).

$$\alpha_{\text{III/IV}} > \Theta_{\text{III/IV}} > \beta_{\text{III/IV}}, \quad (21)$$

where

$$\Theta_{\text{III/IV}} = (\theta_{96}, \theta_{97}). \quad (22)$$

2.8.1 Outliers and Replicability of West Hanauī Solutions

The three chronological solutions for the West Hanauī site did not identify outlier age determinations.

West Hanauī Heaton Set Solution Various measures of boundary estimates for West Hanauī (table 49) vary by thirty or fewer years over five calibrations that use the ΔR value recommended by Heaton et al. (2020). This result indicates that the calibration is replicable.

Table 49: Replicability of Heaton set West Hanauī site chronology solutions

	mean	q1	median	q3	ci.inf	ci.sup
West Hanauī start	19	30	10	6	21	11
West Hanauī end	5	5	7	5	4	1

West Hanauī Burr Set Solution Various measures of boundary estimates for West Hanauī (table 50) vary by 42 or fewer years over five calibrations that use a ΔR estimate based on Burr et al. (2009). This result indicates that the calibration is replicable.

Table 50: Replicability of Burr set West Hanau site chronology solutions

	mean	q1	median	q3	ci.inf	ci.sup
West Hanau start	21	42	12	5	28	11
West Hanau end	6	6	10	6	5	1

West Hanau Conservative Set Solution Various measures of boundary estimates for West Hanau (table 51) vary by 22 or fewer years over five calibrations that use a ΔR estimate based on Burr et al. (2009) incorporating a conservative estimate of the error. This result indicates that the calibration is replicable.

Table 51: Replicability of Conservative set West Hanau site chronology solutions

	mean	q1	median	q3	ci.inf	ci.sup
West Hanau start	12	22	12	7	15	6
West Hanau end	6	6	8	5	6	1

2.8.2 West Hanau Site Chronology Summary

The value of ΔR has no appreciable effect on the chronology of the West Hanau site (table 52), as is expected, given that both age determinations are on wood charcoal. In this situation, any of the three solutions can be used to interpret the chronology of the West Hanau site.

Table 52: Variability in West Hanau site chronology solutions

	mean	q1	median	q3	ci.inf	ci.sup
West Hanau start	4	7	5	3	6	7
West Hanau end	3	4	5	3	3	0

The Conservative set solution is selected here (table 53, fig. 12). The 95% credible interval for West Hanau start is AD 417–1646, and for West Hanau end is AD 1529–1950.

Table 53: Summary statistics for West Hanai site chronology solution

	mean	sd	min	q1	median	q3	max	ci.inf	ci.sup
West Hanai start	1271	331	330	1151	1393	1496	1857	417	1646
West Hanai end	1726	124	1418	1628	1719	1828	1952	1529	1950

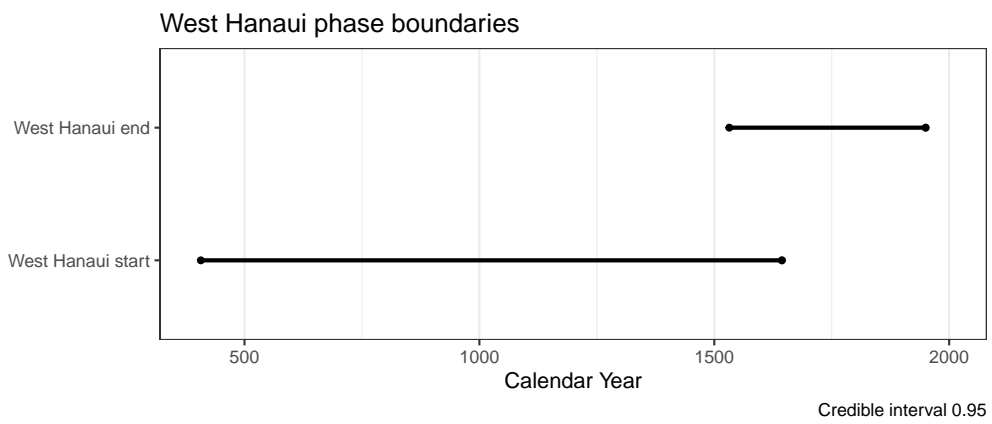


Figure 12: West Hanai phase boundaries, Conservative set.

3 Marquesan Site Chronology Solutions

The status of the eight site chronologies can be assessed by comparing the proportion of age determinations identified as outliers, the variability generated by multiple calibration runs after outliers have been removed, and the influence exercised by the choice of ΔR . These measures indicate in general terms how well the interpretation of site stratification fits the chronological data collected during excavation after outliers have been removed. The results show the positive influence of chronometric hygiene, the practical difficulty of isolating stratigraphic units during excavation in unconsolidated calcareous sand deposits, the tenuous nature of stratigraphic correlations among discontinuous excavation units, and the relatively mild effect of ΔR on estimates of model parameters. Here, we offer a precise set of terms for comparing the intervals represented by the earliest deposits at Hanamiai and other Marquesan sites, and recommendations for future inquiry into the chronology of the eight sites.

3.1 Robust Identification of Outliers

Calibration of chronology solutions did not identify outliers for four sites, including Hakaea, Teavau'ua, East Hanauī, and West Hanauī. For the Hakaea and Teavau'ua sites, this circumstance appears due to the conscientious application of chronometric hygiene and the limited need for stratigraphic correlation. For East Hanauī it appears due to the limited dating program, which processed a single age determination for each stratigraphic unit. For West Hanauī a single phase was excavated, so there are no stratigraphic constraints that might be used to identify outliers.

The two extensively excavated sites, Hanamiai and Hane, yielded relatively few outliers. Two outliers were identified among the 22 age determinations for Hanamiai, both on unidentified charcoal that appears to have included old wood. Seven outliers were identified among the 41 age determinations for Hane, including three age determinations on unidentified charcoal that likely included old wood, two on apparently old pieces of marine shell, and two that appear to be intrusive to the stratigraphic units where they were recovered. These results reflect an early neglect of chronometric hygiene and the easy mobility of materials across site stratification boundaries. Conspicuously absent from this analysis of the Hane age determinations is evidence for systematic error in the age determinations produced by the Gakushūin laboratory, a claim that is often made in Pacific archaeology (Spriggs and Anderson 1993, 207; Anderson 1991, 782–783). Dissatisfaction with dating results from the Gakushūin laboratory first surfaced at the Hālawa Dune site in Hawai'i, where several age determinations could not be distinguished from the modern standard, apparently due to incomplete removal of rootlets during sample pretreatment (Kirch 1975). It resurfaced a decade later in the context of an argument for Polynesian settlement of Eastern Polynesia “as early as the mid-first millennium B.C.” (Kirch 1986, 25), which posited that the age determinations processed by the Washington State University laboratory correctly dated cultural activity

at Hane, and that the Gakushūin dates were too late for their stratigraphic units (see also Rolett 1993, 34). Data collected subsequently contradict this argument, pointing instead to late settlement of Eastern Polynesia about a thousand years ago. These data indicate that the Gakushūin and Washington State University laboratories produced outlier age determinations, as well as age determinations that fit the data and chronological model presented here. According to these data and the model, four of the seven dates from the Washington State University laboratory are identified as outliers that are too old for their stratigraphic units, while three age determinations fit the data and the model. Several age determinations from the Gakushūin laboratory could not be distinguished from the modern standard and were not included in this analysis; these age determinations might point to inadequate laboratory pretreatment, as indicated for the Hālawa Dune site. Inadequate pretreatment might also help explain the two outliers from Gakushūin laboratory identified during the calibrations reported here, both of which are too young for their stratigraphic units. Nevertheless, four age determinations from Gakushūin laboratory fit the data and the model, and appear to date cultural activity correctly at the Hane site. These considerations indicate that the practice of rejecting Gakushūin age determinations as unreliable is likely an over-reaction to sample pretreatment problems that affected some, but not all, of the age determinations produced by that laboratory.

The Ho'oumi chronology developed here depends on a novel site-wide interpretation of the stratification (section 2.5). The single outlier identified from Ho'oumi comes from an age determination on legacy material from Suggs' excavations. As it stands, the outlier appears to indicate that correlation of the paleotsunami deposit across the site is faulty; the correlation works well for the excavations conducted during the 2011 re-investigation of Ho'oumi, but fails when extended inland to Suggs' excavations. Alternatively, the dated material might have been intrusive, even though it was collected in situ from the fill of a hearth, or the dated material might have been mislabeled or stored incorrectly in the laboratory. In any case, this result reinforces the conclusion that the dominance of straight-shank one-piece fishhooks and East Polynesian trolling lure points, dates both of Suggs' Ho'oumi occupations to after AD 1450 (see main text and Supplement 2), and presumably after the paleotsunami.

Finally, there is the Ha'atuatua site where seven age determinations are identified as outliers in a corpus of 21 dates. One contributor to the large numbers of outliers identified for Ha'atuatua is a poor fit of the site stratigraphic model with the actual stratification of the site. Ha'atuatua is a large site that has been excavated with test units and trenches widely separated from one another. In this situation, stratigraphic correlations are difficult to make with certainty because they require uniform stratification over long distances, which is unlikely in a dynamic landform such as Ha'atuatua where the deposits consist of calcareous sand.

3.2 Replicability of Site Chronology Solutions

All three site chronology solutions—the Heaton set, the Burr set, and the Conservative set—are replicable for each of the eight sites, with estimates of stratigraphic unit boundaries that typically vary by a decade or less. This is a testament to the effectiveness of outlier identification and treatment, and to the simplicity of the models, especially at Hane and Hanamiai where stratigraphic units separated by the excavators were subsequently merged to compensate for the vertical movement of materials in the unconsolidated calcareous sand matrix of the sites.

3.3 Effect of Local Marine Reservoir Correction

At this stage of Marquesan chronology building, the choice of a local marine reservoir correction, ΔR , among the various possibilities based on the work of Burr et al. (2009), has a generally negligible effect on site chronology. The observed variability is on the order of a decade or two at sites where marine shell has been dated, and, as expected, less at sites where no marine shell has been dated.

Note that the three ΔR estimates proposed on the basis of “paired” marine and terrestrial samples drawn from Marquesan archaeological sites (Petchey et al. 2009; Allen et al. 2021; Petchey 2020) are each problematic and should be avoided in practice (see section 1.2).

3.4 Relations of the Early Hanamiai Deposit

This section uses the Allen algebra (J. F. Allen 1983) to compare the time interval represented by the early stratigraphic unit, Hanamiai I/II, with other site stratigraphic units, including Hane Lower, Hakaea VII, West Hanau, East Hanau VI, Ho’oumi Phase A/B, Ha’atuatua C and Teavau’ua IV (fig. 13). The comparison of intervals establishes English language terms that describe their relationships consistently.

Given the model and the data, Hanamiai was settled after other locations in the Marquesas. Deposition of Hanamiai I/II was overlapped by deposition of Hane Lower and during deposition of Ha’atuatua C, Ho’oumi A/B, and East Hanau VI, although this latter relation is strongly influenced by the sparse information for East Hanau.

Hanamiai appears to have been settled before other locations in the Marquesas. Deposition of Hanamiai I/II likely contains deposition of Hakaea VII, and likely contains or overlaps deposition of Teavau’ua IV. It likely precedes deposition at West Hanau, although the sparse information from that site makes other relations possible, as well.

4 Marquesan Chronology

The first part of this section summarizes the rate at which Polynesians established settlements in the Marquesas. This topic is investigated with an occurrence plot model based

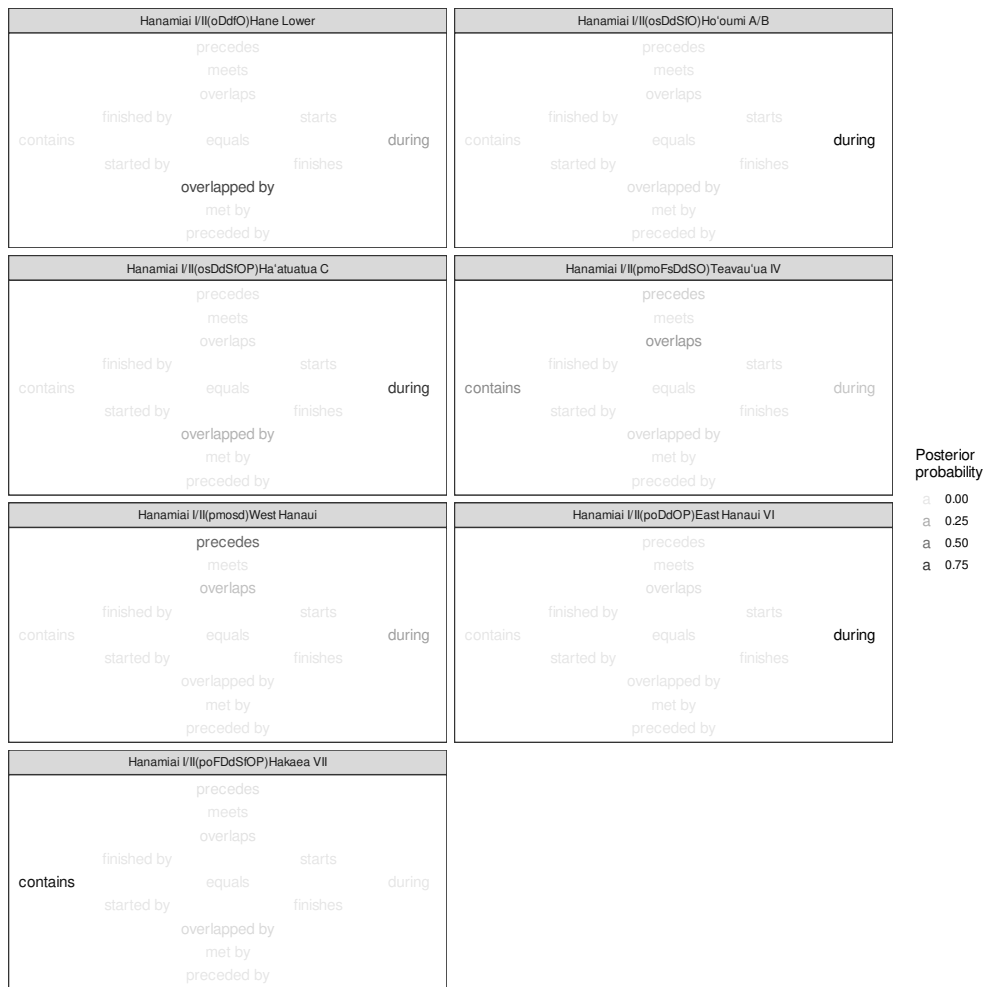


Figure 13: Relation of Hanamiai I/II to other stratigraphic units, based on results of the Conservative set. See fig. 3 for an illustration of Allen relations.

on site chronology solutions for the six best-documented early sites set out in section 3. The second part of this section builds a chronological model for Marquesan material culture change using the Chronomodel application.

4.1 Polynesian Settlement History of the Marquesas

The settlement history of the Marquesas is approached here from an archipelago-wide perspective, with data from the islands of Tahuata, Ua Huka, and Nuku Hiva. Age estimates for the lower boundaries of the basal cultural deposits at six relatively well-dated sites are used to construct an occurrence plot (fig. 14). Instead of asking if a particular site, such as Hanamiai, was settled before or after some other site, such as

Hane, the occurrence plot illustrates the rate at which site establishment progressed from the first to the sixth settlement, without regard to which specific site is ranked first, second, third and so on in the sequence. Data for this analysis derives from Hanamiai I/II (see table 7), Hane Lower (see table 14), Hakaea VII (see table 20), Ha'atuatua C (see table 41), Teavau'ua IV (see table 26), and Ho'oumi A/B (see table 33).

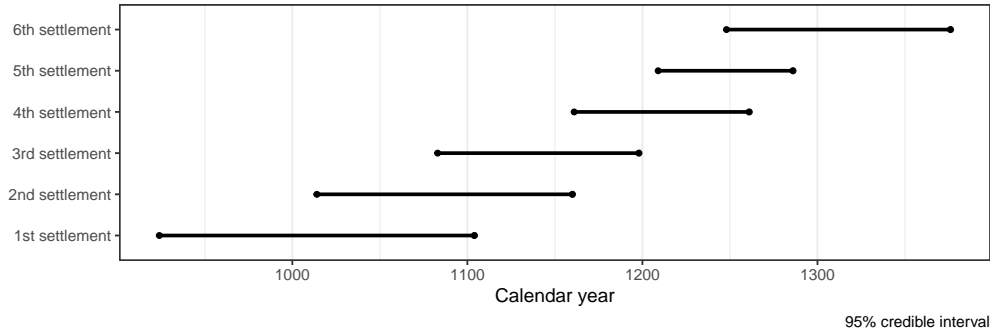


Figure 14: Marquesan settlement history based on chronologies from six relatively well-dated early sites.

Given the model and the data, the Marquesas were first settled around the turn of the second millennium, in AD 931–1102 (table 54). The second settlement was established about a century later, in AD 1016–1160. The third settlement, established in AD 1083–1199, is followed by the fourth in AD 1161–1261, the fifth in AD 1210–1287, and the sixth in AD 1250–1377.

Table 54: Summary statistics for Marquesan settlement history

	mean	sd	min	q1	median	q3	max	ci.inf	ci.sup
1	998	43	628	976	994	1012	1136	924	1104
2	1098	41	881	1071	1106	1129	1182	1014	1160
3	1142	27	970	1129	1145	1157	1255	1083	1198
4	1215	26	1075	1200	1218	1234	1280	1161	1261
5	1252	23	1107	1238	1254	1267	1377	1209	1286
6	1289	37	1185	1269	1277	1287	1384	1248	1376

4.2 Material Culture Change

This section experiments with a method new to Pacific archaeology that distinguishes the event time of site chronology and the substance time of artifact occurrence to investigate material culture change (Dye et al. 2023). The goal of this particular experiment is to estimate when artifact assemblages characterized as East Polynesian Archaic, or Archaic, transformed to assemblages characterized as Classic Marquesan, or Classic. Distinctive

Archaic assemblages were recognized informally for many years before they were so-named by Sinoto in 1981 (Kirch 1986, 16). East Polynesian Archaic assemblages are characterized by a wide range of distinctive artifacts, many of which are either rare or appear to have restricted geographical distributions, making it difficult for analysts to identify which elements comprise the defining characteristics.

At times, the goal of determining which of the possible Archaic assemblages “do or do not belong” has been described as a seemingly insurmountable challenge (Walter 1996, 515). Notably, however, a large collection of well-provenanced artifacts from the Hanamiai North and South excavations now offers potential for overcoming the impasse described by Walter. The three-step approach taken here consists of: (i) identifying temporally-sensitive artifacts in the Hanamiai assemblages; (ii) using this evidence to distinguish among the Archaic, Classic and Historic era Hanamiai assemblages; and (iii) using the same criteria to identify Archaic and Classic artifact assemblages for some of the other sites included in our study. Certain sites were excluded from the Archaic/Classic transition model because the artifact assemblages have not been reported in detail or because of uncertainty in relating the site’s chronological data to the artifact assemblages. The rationale for including or excluding specific sites is explained in the Supplement 2 site summaries.

Although our Archaic/Classic transition model focuses on the Marquesas, a similar approach might be extended to other islands such as New Zealand, the Cooks and the Societies. Varying degrees of interaction and exchange shaped early developments in these East Polynesian archipelagoes. Across this vast area, however, the archaeological evidence shows a general decline over time in interaction (e.g. Rolett 1998, 2002; Walter 1996; Weisler 2002). In the Marquesas and elsewhere, Archaic artifact traditions eventually became obsolete, when they either fell out of use completely or were replaced by a distinctive local tradition that differed from the traditions developed elsewhere within the geographic range of the Archaic. Despite the difficulties introduced by rare specimens and restricted geographic distributions, this process signals the differentiation of an early widespread community of culture into the diverse, but closely related, Polynesian cultures encountered by European explorers in the sixteenth through eighteenth centuries (Walter 1996, 522). Thus, estimating the timing of a transition from an Archaic to a Classic artifact assemblage represents a useful first step for an inquiry that seeks to characterize when and how a distinctively Marquesan material culture developed.

The Marquesan artifacts in our study were mostly collected from stratigraphic contexts that were laid down over extended periods of time. This situation sets certain limits on an investigation of artifact change (Perreault 2019). In particular, if the process of artifact change took place over an interval of time shorter than the stratigraphic contexts that yielded the artifacts, then the artifact assemblages will undersample the process of artifact change. In practical terms, this means that the analysis of artifact change cannot be carried out with the goal of identifying and describing a detailed process. Instead, a coarser-grained model is required—one with the more limited goal of estimating when

one kind of assemblage class transitioned to another kind of assemblage class. This compromise, which imposes a strong model assumption to make up for the under-determination of the artifact sample, is not ideal but will be necessary until artifact-rich deposits with higher temporal resolution are identified and excavated. Nevertheless, our experimental model provides building blocks that future researchers might adapt and re-use to construct more detailed models of change.

The model offered here works at the level of the assemblage. It aims to identify a point in time for the transition of one assemblage class to another, rather than describing a detailed process of change in particular artifact classes. The model assumes transformative change, where an Archaic artifact assemblage at time t is transformed to a Classic artifact assemblage at time $t + 1$. Moreover, the model assumes that it is possible to identify the necessary and sufficient conditions for assigning an artifact assemblage to one of the two classes, Archaic or Classic (table 55). In addition to the Archaic/Classic transition, transitions of the component artifact types are also calculated. These include estimates for the transitions from Archaic West Polynesian lures, curved or angular-shank fishhooks, and untanged adzes to Classic East Polynesian lures, straight-shank fishhooks, and tanged adzes. Like the assemblage transition, these transitions are also modeled as transformative. Stratigraphic contexts for the sites in our study were assigned to the Archaic and Classic periods based on the abundance, presence, and absence of temporally diagnostic artifacts (table 55). The Hanamiai III transitional assemblage was initially classified as Archaic, and this is the calibration summarized below. Subsequently, a new calibration was constructed in which the Hanamiai III transitional assemblage was classified as Classic, with the goal of estimating the sensitivity of the model with respect to classification of the transitional assemblage. Results of this calibration and a comparison of transition estimates can be found at the end of this section. The Bayesian calibration application `Chronomodel` (Lanos et al. 2015) was selected for this analysis because it is designed expressly for modeling artifact change.

`Chronomodel` differs from the `BCal` (Buck, Christen, and James 1999) and `OxCal` (Ramsey 1995) applications, which are designed to model site chronologies as well as artifact change, but which require special care when modeling artifact change. This is because both `BCal` and `OxCal` typically apply a uniformity assumption and squeezing routine that work together to counteract the effect of statistical scatter on stratigraphic phase-boundary age estimates (Nicholls and Jones 2001). However, although statistical scatter is a particular concern in modeling site chronologies, it is not an issue in modeling depositional histories of artifacts. Rather, the concern with artifacts is that the temporal range of an observed artifact depositional history underestimates the true temporal range due to preservation bias and sampling error (Perreault 2019, 101–104). Also, when modeling artifact change, the absolute age of a change in the qualities and relations of artifacts is best estimated by the associated age determination(s), absent the temporal adjustments of individual age determinations required to counteract the effect of statistical scatter on stratigraphic phase boundaries. `Chronomodel` makes it easy to

Table 55: Abundance, presence, and absence of temporally diagnostic artifacts

	Hanami I/II	Hanami III	Hanami IV	Hane Lower	Hane Upper	Ha'atuatua B	Hakaea VII/V	E. Hanau VI	E. Hanau II	W. Hanau
	Archaic	Transitional	Classic	Archaic	Classic	Archaic	Archaic	Archaic	Classic	Classic
Fishhook shank										
Curved or angular	++ ^a	++	+ ^b	++	- ^c	++	+	++	-	-
Straight	+	+	++	+	+	+	-	+	+	+
Trolling lures										
"West Polynesian"	+	-	-	+	-	+	-	-	-	-
"East Polynesian"	-	-	+	-	-	-	-	-	-	-
Adzes										
Untanged	+	-	-	++	-	++	-	-	-	-
Tanged	-	-	+	+	+	+	-	-	-	-
Breadfruit culture										
Cowrie-shell peeler	-	-	+	-	-	-	-	-	-	-
Poi pounder	-	-	-	-	+	-	-	-	-	-

a. dominant

b. present

c. absent

carry out an analysis of artifact change that is not unduly influenced by the uniformity assumption and squeezing routine. In contrast, special care must be taken to achieve similar results in either OxCal or BCal (Banks et al. 2019, 207–211).

In order to achieve this ease of use, Chronomodel introduces a novel approach to calibration known as the event date model (Lanos and Philippe 2018), and it employs an algorithm that automatically handles statistical outliers, thus relieving the analyst of the tasks related to identifying and removing outliers. These differences raise the question whether or not the results of a Chronomodel calibration are comparable to the results of a calibration run in OxCal or BCal. In the case of the Marquesan site chronologies, this question can be addressed by comparing the site chronologies in Section 3, generated by OxCal, with the results of a Chronomodel calibration designed to replicate the OxCal analysis. In general, the results differ considerably when the estimate is unconstrained, as it is at the beginning of a stratigraphic sequence. The differences are less pronounced when the estimate is constrained, but they still range to a hundred years or more, as can be seen by comparing Figure 5 with Figure 15.

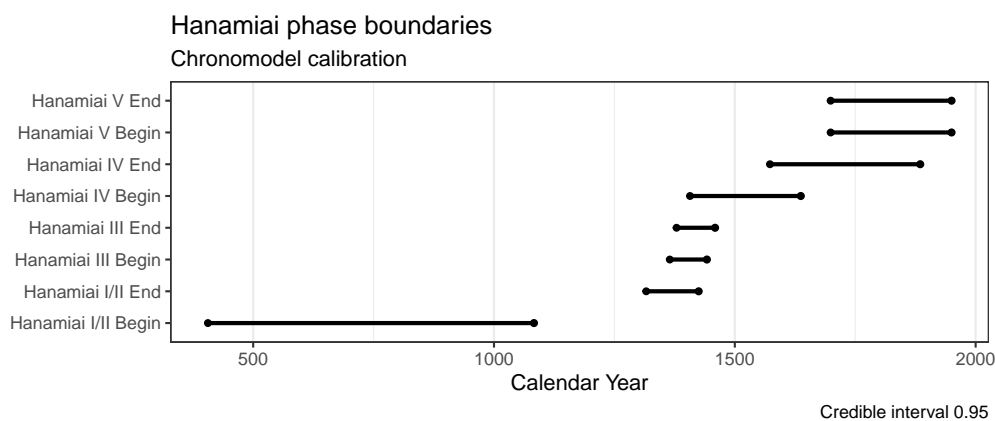


Figure 15: Hanamiai phase boundaries, Chronomodel calibration. Compare to Figure 5.

Marquesan artifact traditions appear to have undergone a period of change in the late fourteenth and fifteenth centuries (table 56). Given the data and a model that assigns the Hanamiai transitional deposit to the Archaic period, the transition from Archaic to Classic assemblages was underway in AD 1386–1474 (table 57). When the Hanamiai transitional deposit is assigned to the Classic period, the estimate is AD 1369–1449 (table 58). Most of the artifact sequences, including adzes, fishhooks, and breadfruit culture, are in transition at this time, as well. The transition to an East Polynesian lure might have occurred somewhat later, and is estimated at AD 1373–1636 (table 57) or AD 1361–1634 (table 58). These transition estimates might serve as useful points of reference for regional comparisons.

Estimates for transitions in artifact assemblages are mildly sensitive with respect to

Table 56: Summary statistics of Marquesan artifact traditions

	mean	sd	min	q1	median	q3	max	ci.inf	ci.sup
Archaic Begin	256	155	0	130	244	367	819	0	526
Archaic End	1406	18	1331	1393	1406	1418	1480	1371	1442
Classic Begin	1412	18	1344	1400	1412	1425	1490	1377	1450
Classic End	1815	75	1550	1761	1816	1875	1950	1687	1950
Tanged adzes Begin	1430	20	1349	1417	1430	1443	1537	1391	1468
Tanged adzes End	1777	79	1526	1719	1774	1832	1950	1640	1936
Untanged adzes Begin	257	155	0	131	245	368	829	0	529
Untanged adzes End	1398	20	1300	1384	1398	1412	1480	1358	1437
West Polynesian lure Begin	257	155	0	131	245	368	829	0	529
West Polynesian lure End	1405	19	1331	1393	1405	1418	1480	1369	1442
East Polynesian lure Begin	1506	64	1364	1457	1494	1543	1834	1406	1639
East Polynesian lure End	1726	80	1446	1672	1728	1782	1949	1570	1882
Curved shank hooks dominant Begin	256	155	0	130	244	367	819	0	527
Curved shank hooks dominant End	1421	19	1345	1408	1421	1433	1517	1384	1458
Straight shank hooks dominant Begin	1430	20	1349	1417	1430	1443	1537	1391	1468
Straight shank hooks dominant End	1850	67	1559	1806	1860	1905	1950	1725	1950
Breadfruit culture Begin	1430	20	1349	1417	1430	1443	1537	1391	1468
Breadfruit culture End	1850	67	1559	1806	1860	1905	1950	1725	1950

Table 57: Transition estimates when the transitional assemblage is classified as Archaic

Transition	95% Credible Interval
Archaic to Classic	AD 1386–1474
Untanged to tanged adze	AD 1358–1477
West Polynesian to East Polynesian lure	AD 1373–1636
Curved shank to straight shank fishhooks	AD 1384–1474
Breadfruit culture begins	AD 1394–1475

Table 58: Transition estimates when the transitional assemblage is classified as Classic

Transition	95% Credible Interval
Archaic to Classic	AD 1369–1449
Untanged to tanged adze	AD 1359–1472
West Polynesian to East Polynesian lure	AD 1361–1634
Curved shank to straight shank fishhooks	AD 1382–1468
Breadfruit culture begins	AD 1395–1476

classification of the Hanamiai III transitional assemblage as either Archaic or Classic. Assigning the Hanamiai III transitional assemblage to the Classic period yields transition estimates that are somewhat earlier than estimates when the transitional assemblage is assigned to the Archaic period. Nevertheless, the differences are typically small. Comparing the entries in Table 57 with those in Table 58 indicates that the largest difference is the estimate for the transition from Archaic to Classic, which shifts 15–25 years. The other transitions differ by less than a decade.

Input Files

The OxCal input files for the Marquesas calibrations are embedded as file attachments in this PDF document. Links to the files are presented in Table 59. These files can be accessed with a PDF reader application, such as Adobe Acrobat Reader or Microsoft Edge, that recognizes file attachments.

Table 59: OxCal input files for the Marquesas calibrations

File name	Link to file
marquesas_burr.oxcal	Extract file
marquesas_conservative.oxcal	Extract file
marquesas_heaton.oxcal	Extract file

The Chronomodel input files are embedded as file attachments in this PDF document. Links to the files are presented in Table 60. These files can be accessed with a PDF reader application, such as Adobe Reader or Microsoft Edge, that recognizes file attachments.

Table 60: Chronomodel input files for the Marquesas calibrations

File name	Link to file
mqs_final_htt.chr	Extract file
mqs_final_classic_htt.chr	Extract file

References

- Allen, James F. 1983. "Maintaining knowledge about temporal intervals." *Communications of the ACM* 26 (11): 832–843.
- Allen, Melinda S. 2004. "Revisiting and revising Marquesan culture history: New archaeological investigations at Anaho Bay, Nuku Hiva Island." *Journal of the Polynesian Society* 113 (2): 143–196.
- . 2014. "Marquesan colonisation chronologies and post-colonisation interaction: Implications for Hawaiian origins and the 'Marquesan homeland' hypothesis." *Journal of Pacific Archaeology* 5 (2): 1–17.
- Allen, Melinda S., William R. Dickinson, and Jennifer M. Huebert. 2012. "The anomaly of Marquesan ceramics: A fifty year retrospective." *Journal of Pacific Archaeology* 3 (1): 90–104.
- Allen, Melinda S., and Jennifer M. Huebert. 2014. "Short-lived plant materials, long-lived trees, and Polynesian ¹⁴C dating: Considerations for ¹⁴C sample selection and documentation." *Radiocarbon* 56 (1): 257–276.
- Allen, Melinda S., Tara Lewis, and Nick Porch. 2022. "Lost bioscapes: Floristic and arthropod diversity coincident with 12th century Polynesian settlement, Nuku Hiva, Marquesas Islands." *PLoS ONE* 17 (3): e0265224. <https://doi.org/https://doi.org/10.1371/journal.pone.0265224>.
- Allen, Melinda S., Andrew McAlister, Fiona Petchey, Jennifer M. Huebert, Ma'ara Maeva, and Benjamin D. Jones. 2021. "Marquesan ceramics, palaeotsunami, and megalithic architecture: Ho'oumi Beach site (NHo-3) in regional perspective." *Archaeology in Oceania*, <https://doi.org/10.1002/arco.5233>.
- Allen, Melinda S., and Andrew J. McAlister. 2010. "The Hakaea Beach site, Marquesan colonisation, and models of East Polynesian settlement." *Archaeology in Oceania* 45:54–65.
- Alspaugh, Thomas A. 2019. "Allen's Interval Algebra." <https://www.thomasalspaugh.org/pub/fnd/allen.html>.
- Anderson, Atholl. 1991. "The chronology of colonization in New Zealand." *Antiquity* 65:767–795.

- Anderson, Atholl. 1994. "Palaeoenvironmental evidence of island colonization: A response." *Antiquity* 68:845–847.
- Anderson, Atholl, John Chappell, Michael Gagan, and Richard Grove. 2006. "Prehistoric maritime migration in the Pacific islands: an hypothesis of ENSO forcing." *The Holocene* 16 (1): 1–6.
- Anderson, Atholl, and Yosihiko H. Sinoto. 2002. "New radiocarbon ages of colonization sites in East Polynesia." *Asian Perspectives* 41 (2): 242–257.
- Athens, J. Stephen, Timothy M. Rieth, and Thomas S. Dye. 2014. "A paleoenvironmental and archaeological model-based age estimate for the colonization of Hawai'i." *American Antiquity* 79 (1): 144–155.
- Baillie, M. G. L. 1990. "Checking back on an assemblage of published radiocarbon dates." *Radiocarbon* 32:361–366.
- Banks, William E., Pascal Bertran, Sylvain Ducasse, Laurent Klaric, Philippe Lanos, Caroline Renard, and Miriam Mesa. 2019. "An application of hierarchical Bayesian modeling to better constrain the chronologies of Upper Paleolithic archaeological cultures in France between ca. 32,000–21,000 calibrated years before present." *Quaternary Science Reviews* 220:188–214.
- Bayliss, Alex. 2009. "Rolling out revolution: Using radiocarbon dating in archaeology." *Radiocarbon* 51 (1): 123–147.
- . 2015. "Quality in Bayesian chronological models in archaeology." *World Archaeology* 47 (4): 677–700.
- Bayliss, Alex, Shahina Farid, and Thomas Higham. 2014. "Time will tell: Practicing Bayesian chronological modeling on the East Mound." In *Çatalhöyük Excavations: The 2000–2008 Seasons*, edited by Ian Hodder, 53–90. BIAA Monograph 46. Monumenta Archaeologica 29. London, UK and Los Angeles, CA: British Institute at Ankara / Cotsen Institute of Archaeology Press.
- Bayliss, Alex, and Christopher Bronk Ramsey. 2004. "Pragmatic Bayesians: A decade of integrating radiocarbon dates into chronological models." Chap. 2 in *Tools for Constructing Chronologies: Crossing Disciplinary Boundaries*, edited by Caitlin E. Buck and Andrew R. Millard, 25–41. Lecture Notes in Statistics 177. London: Springer.
- Bellwood, Peter S. 2013. *First Migrants: Ancient Migration in Global Perspective*. Chichester UK: Wiley Blackwell.
- Bronk Ramsey, Christopher. 2008. "Radiocarbon dating: Revolutions in understanding." *Archaeometry* 50 (2): 249–275.
- . 2009a. "Bayesian analysis of radiocarbon dates." *Radiocarbon* 51 (1): 337–360.

- Bronk Ramsey, Christopher. 2009b. "Dealing with outliers and offsets in radiocarbon dating." *Radiocarbon* 51 (3): 1023–1045.
- Buck, Caitlin E., William G. Cavanagh, and Clifford D. Litton. 1996. *Bayesian Approach to Interpreting Archaeological Data*. Statistics in Practice. Chichester, UK: John Wiley & Sons.
- Buck, Caitlin E., J. Andrés Christen, and Gary N. James. 1999. "BCal: An on-line Bayesian radiocarbon calibration tool." *Internet Archaeology* 7. <http://intarch.ac.uk/journal/issue7/buck/>.
- Buck, Caitlin E., and Bo Meson. 2015. "On being a good Bayesian." *World Archaeology* 47 (4): 567–584.
- Burr, G. S., J. W. Beck, Thierry Corrège, G. Cabioch, F. W. Taylor, and D. J. Donahue. 2009. "Modern and Pleistocene reservoir ages inferred from South Pacific corals." *Radiocarbon* 51 (1): 319–335.
- Chamberlin, T. C. 1965. "The method of multiple working hypotheses." *Science* 148 (3671): 754–759.
- Christen, J. Andrés. 1994. "Summarizing a set of radiocarbon determinations: A robust approach." *Applied Statistics* 43 (3): 489–503.
- Conte, Eric, and Guillaume Molle. 2014. "Reinvestigating a key site for Polynesian prehistory: New results from the Hane dune site, Ua Huka (Marquesas)." *Archaeology in Oceania* 49:121–136.
- Dean, Jeffrey S. 1978. "Independent dating in archaeological analysis." In *Advances in Archaeological Method and Theory*, edited by M. B. Schiffer, 1:223–265. New York: Academic Press.
- Dye, Thomas S. 2000. "Effects of ^{14}C sample selection in archaeology: An example from Hawai'i." *Radiocarbon* 42 (2): 203–217.
- . 2011. "A model-based age estimate for Polynesian colonization of Hawai'i." *Archaeology in Oceania* 46:130–138.
- . 2015. "Dating human dispersal in Remote Oceania: A Bayesian view from Hawai'i." *World Archaeology* 47 (4): 661–676.
- Dye, Thomas S., and Caitlin E. Buck. 2015. "Archaeological sequence diagrams and Bayesian chronological models." *Journal of Archaeological Science* 63:84–93.
- Dye, Thomas S., Caitlin E. Buck, Robert J. DiNapoli, and Anne Philippe. 2023. "Bayesian chronology construction and substance time." *Journal of Archaeological Science* 153:105765.
- Elliot, Louis P., and Barry W. Brook. 2007. "Revisiting Chamberlin: Multiple working hypotheses for the 21st century." *BioScience* 57 (7): 608–614.

- Harris, Edward C. 1989. *Principles of Archaeological Stratigraphy*. Second. London: Academic Press.
- Heaton, Timothy J., Peter Köhler, Martin Butzin, Edouard Bard, Ron W. Reimer, William E. N. Austin, Christopher Bronk Ramsey, et al. 2020. "Marine20—the marine radiocarbon age calibration curve (0–55,000 cal BP)." *Radiocarbon* 62 (4): 779–820.
- Kirch, Patrick V. 1975. "Excavations at sites A1–3 and A1–4: Early settlement and ecology in Halawa Valley." In *Prehistory and Ecology in a Windward Hawaiian Valley: Halawa Valley, Molokai*, edited by Patrick Vinton Kirch and Marion Kelly, 17–70. Pacific Anthropological Records 24. Honolulu: Anthropology Department, B. P. Bishop Museum.
- . 1986. "Rethinking East Polynesian prehistory." *Journal of the Polynesian Society* 95:9–40.
- Komugabe-Dixon, Aimée F., Stewart J. Fallon, Stephen M. Eggins, and Ronald E. Thresher. 2016. "Radiocarbon evidence for mid-late Holocene changes in southwest Pacific Ocean circulation." *Paleoceanography and Paleoclimatology* 31 (7): 971–985. <https://doi.org/10.1002/2016PA002929>.
- Lanos, Ph., A. Philippe, H. Lanos, and Ph. Dufresne. 2015. *Chronomodel: Chronological Modelling of Archaeological Data using Bayesian Statistics*. <http://www.chromodel.fr>.
- Lanos, Philippe, and Anne Philippe. 2018. "Event date model: a robust Bayesian tool for chronology building." *Communications for Statistical Applications and Methods* 25 (2): 131–157.
- Nicholls, Geoff, and Martin Jones. 2001. "Radiocarbon dating with temporal order constraints." *Journal of the Royal Statistical Society: Series C (Applied Statistics)* 50 (4): 503–521.
- Paris, Raphaël, Simon Falvard, Catherine Chagué, James Goff, Samuel Etienne, and Pascal Doumalin. 2020. "Sedimentary fabric characterized by X-ray tomography: A case study from tsunami deposits on the Marquesas Islands, French Polynesia." *Sedimentology* 67:1207–1229. <https://doi.org/10.1111/sed.12582>.
- Paterne, Martine, Linda K Ayliffe, Maurice Arnold, Guy Cabioch, Nadine Tisnérat-Laborde, Christine Hatté, Eric Douville, and Edouard Bard. 2004. "Paired ^{14}C and $^{230}\text{Th}/\text{U}$ dating of surface corals from the Marquesas and Vanuatu (Sub-Equatorial Pacific) in the 3000 to 15,000 cal yr interval." *Radiocarbon* 46 (2): 551–566. <https://doi.org/10.1017/S0033822200035608>.
- Perreault, Charles. 2019. *The Quality of the Archaeological Record*. Chicago, IL: University of Chicago Press.

- Petchey, Fiona. 2020. "New evidence for a mid- to late-Holocene change in the marine reservoir effect across the South Pacific gyre." *Radiocarbon* 62 (1): 127–139.
- Petchey, Fiona, Melinda S. Allen, David J. Addison, and Atholl Anderson. 2009. "Stability in the South Pacific surface marine ¹⁴C reservoir over the last 750 years. Evidence from American Samoa, the southern Cook Islands and the Marquesas." *Journal of Archaeological Science* 36:2234–2243.
- Petchey, Fiona, and Magdalena M. E. Schmid. 2020. "Vital evidence: Change in the marine ¹⁴C reservoir around New Zealand (Aotearoa) and implications for the timing of Polynesian settlement." *Scientific Reports* 10. <https://doi.org/10.1038/s41598-020-70227-3>.
- Philippe, Anne, and Marie-Anne Vibet. 2019. *ArchaeoPhases: Post-Processing of the Markov Chain Simulated by 'ChronoModel', 'Oxcal' or 'BCal'*. R package version 1.4. <https://CRAN.R-project.org/package=ArchaeoPhases>.
- Ramsey, Christopher Bronk. 1995. "Radiocarbon calibration and analysis of stratigraphy: The OxCal program." In *Proceedings of the 15th International ¹⁴C Conference*, edited by G. T. Cook, D. D. Harkness, B. F. Miller, and E. M. Scott, 37:425–430. Radiocarbon.
- Rieth, Timothy M., and Ethan E. Cochrane. 2018. "The chronology of colonization in Remote Oceania." In *The Oxford Handbook of Prehistoric Oceania*, edited by Ethan E. Cochrane and Terry L. Hunt. New York, NY: Oxford University Press.
- Rolett, Barry V. 1993. "Marquesan prehistory and the origins of East Polynesian culture." *Journal de la Société des Océanistes* 96:29–47.
- . 1998. *Hanamiai: Prehistoric Colonization and Cultural Change in the Marquesas Islands (East Polynesia)*. Yale University Publications in Anthropology 81. New Haven, CT: Department of Anthropology / The Peabody Museum, Yale University.
- . 2002. "Voyaging and interaction in ancient East Polynesia." *Asian Perspectives* 41:182–194.
- . 2021. "Results of the 1998, 2001, 2008, 2010, 2012, 2013 and 2014 excavations at the Hanamiai archaeological site, Tahuata, Marquesas Islands." In *Bilan de la recherche archéologique en Polynésie française 2005–2015*, edited by L. T. Anatauarii, 267–275. Dossier d'archéologie Polynésienne 6. Tahiti: Direction de la culture et du patrimoine.
- Rolett, Barry V., and Eric Conte. 1995. "Renewed investigation of the Ha'atuatua dune (Nukuhiva, Marquesas Islands): A key site in Polynesian prehistory." *Journal of the Polynesian Society* 104 (2): 195–228.

- Sinoto, Yosihiko H. 1966. "A tentative prehistoric cultural sequence in the Northern Marquesas Islands, French Polynesia." *Journal of the Polynesian Society* 75 (3): 286–303.
- . 1968. "Position of the Marquesas Islands in East Polynesian prehistory." In *Prehistoric Culture in Oceania: A Symposium*, edited by Ichiro Yawata and Yosihiko H. Sinoto, 111–118. Honolulu: Bishop Museum Press.
- . 1970. "An archaeologically based assessment of the Marquesas Islands as a dispersal center in East Polynesia." In *Studies in Oceanic Culture History*, edited by Roger C. Green and Marion Kelly, 105–132. Pacific Anthropological Records 11. Honolulu: Anthropology Department, B. P. Bishop Museum.
- . 1979. "The Marquesas." In *The Prehistory of Polynesia*, edited by Jesse D. Jennings, 110–134. Cambridge, MA: Harvard University Press.
- Spriggs, Matthew, and Atholl Anderson. 1993. "Late colonization of East Polynesia." *Antiquity* 67:200–217.
- Steadman, David W., and Barry Rolett. 1996. "A chronostratigraphic analysis of landbird extinction on Tahuata, Marquesas Islands." *Journal of Archaeological Science* 23:81–94.
- Stuiver, M., and H. A. Polach. 1977. "Discussion: Reporting of ¹⁴C data." *Radiocarbon* 19:355–363.
- Stuiver, Minze, G. W. Pearson, and T. Braziunas. 1986. "Radiocarbon age calibration of marine samples back to 9000 cal BP." *Radiocarbon* 28 (2B): 980–1021.
- Suggs, Robert C. 1961. *The Archaeology of Nuku Hiva, Marquesas Islands, French Polynesia*. Vol. 49. Anthropological Papers 1. New York, NY: American Museum of Natural History.
- Taylor, R. E. 1987. *Radiocarbon Dating: An Archaeological Perspective*. New York: Academic Press.
- Tuggle, H. David, and Matthew Spriggs. 2001. "The age of the Bellows Dune Site, O18, O'ahu, Hawai'i, and the antiquity of Hawaiian colonization." *Asian Perspectives* 39 (1–2): 165–188.
- Walter, Richard. 1996. "What is the East Polynesian 'Archaic'? A view from the Cook Islands." In *Oceanic Culture History: Essays in Honour of Roger Green*, edited by Janet M. Davidson, Geoffrey Irwin, B. Foss Leach, Andrew K. Pawley, and Dorothy Brown, 513–529. New Zealand Journal of Archaeology Special Publication. Dunedin North, NZ: New Zealand Journal of Archaeology.
- Weisler, Marshall I. 2002. "Centrality and the collapse of long-distance voyaging in East Polynesia." In *Geochemical Evidence for Long-Distance Exchange*, edited by Michael D. Glasscock, 257–273. Westport, CT: Bergin / Garvey.

Whittle, A.W.R., F. Healy, A. Bayliss, and M.J. Allen. 2011. *Gathering Time: Dating the Early Neolithic Enclosures of Southern Britain and Ireland*. Oxford: Oxbow Books.

Whittle, Alasdair, Alex Bayliss, and Frances Healy. 2010. "Event and short-term process." In *Eventful Archaeologies*, edited by Douglas J. Bolender, 68–87. Albany, NY: SUNY Press.

Acknowledgments

Christopher Bronk Ramsey and Ray Kidd offered advice on the structure of OxCal models that greatly facilitated the analysis, in particular addition of an upper bound at AD 1950. Later, Andrew Millard and Christopher Bronk Ramsey offered good advice on how to detect outliers with OxCal, which made possible an implementation of the robust practices advocated by Christen (1994) and familiar to a user of the BCal application. Melinda Allen kindly corresponded on several aspects of her work in the Marquesas, and helped us understand the status of inquiry into the chronology of the Ho'oumi site. Two anonymous reviewers offered suggestions that improved the work; one reviewer's deep knowledge of Nuku Hiva archaeology led the authors to revise their chronological model for Ho'oumi. The authors thank them all for their collegiality. Errors of fact or interpretation rest solely with the authors.